AD_____

CONTRACT NO: DAMD 17-86-C-6084

TITLE: Millimeter Wave Ocular Research

PRINCIPAL INVESTIGATOR: John R. Trevithick, PhD.

CONTRACTING ORGANIZATION: The University of Western Ontario
London, Ontario Canada N6A 5C1

REPORT DATE: September 30, 1995

TYPE OF REPORT: Final

PREPARED FOR: U.S. Army Medical Research and Materiel Command
Fort Detrick
Frederick, Maryland 21702-5012

DISTRIBUTION STATEMENT: Approved for public release;
distribution unlimited

The views, opinions and/or findings contained in this report are those of the author(s) and should not be construed as an official Department of the Army position, policy or decision unless so designated by other documentation.

DISCLAIMER NOTICE

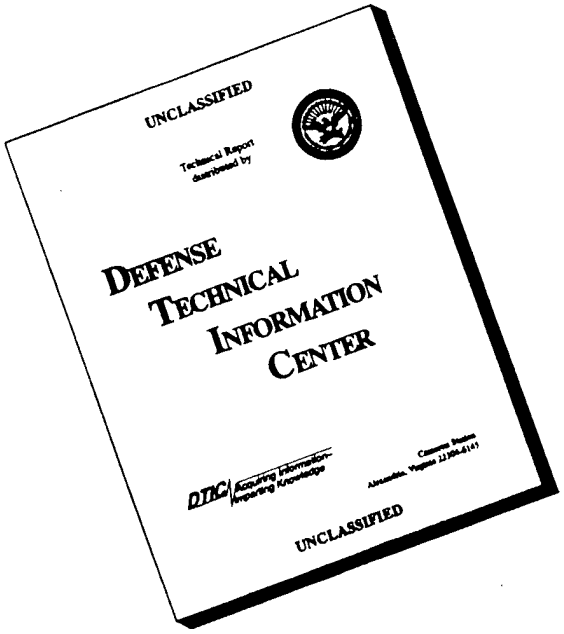

THIS DOCUMENT IS BEST QUALITY AVAILABLE. THE COPY FURNISHED TO DTIC CONTAINED A SIGNIFICANT NUMBER OF PAGES WHICH DO NOT REPRODUCE LEGIBLY.

REPORT DOCUMENTATION PAGE

Form Approved
OMB No. 0704-0188

1. AGENCY USE ONLY (Leave blank)	2. REPORT DATE	3. REPORT TYPE AND DATES COVERED
	Sept. 30, 1995	Final 1 Jan 86 - 30 Dec 88

4. TITLE AND SUBTITLE
Millimeter Wave Ocular Research

5. FUNDING NUMBERS
DAMD17-86-C-6084

6. AUTHOR(S)
John R. Trevithick, Ph.D.

7. PERFORMING ORGANIZATION NAME(S) AND ADDRESS(ES)
University of Western Ontario
London, Ontario, CANADA N6A 5B8

8. PERFORMING ORGANIZATION REPORT NUMBER

9. SPONSORING / MONITORING AGENCY NAME(S) AND ADDRESS(ES)
U.S. Army Medical Research and Materiel Command
Fort Detrick, Maryland 21702-5012

10. SPONSORING / MONITORING AGENCY REPORT NUMBER

11. SUPPLEMENTARY NOTES

12a. DISTRIBUTION / AVAILABILITY STATEMENT
Approved for public release, distribution unlimited

12b. DISTRIBUTION CODE

13. ABSTRACT *(Maximum 200 words)*

Techniques were developed for irradiation of rabbit eyes with 35 GHz millimeter waves to determine cellular damage mechanism and thresholds. The irradiation was performed using anaesthetized 2.5 kg New Zealand white rabbits exposed to 35 GHz pulsed and continuous wave (CW) irradiation delivered by a special focusing antenna to a spot approximately 1.3 cm diameter in which the rabbit eye was placed. The peak specific absorption rate (SAR) (1.4 mW/g per 1 mW/Cm^2 of incident power) was determined with the aid of a thermographic camera which gave a map of the local corneal surface temperatures; the SAR assumed the values of thermal conductivity and specific heat for water since the cornea contains so much water. The damage observed has been divided into four categories which are progressively increased, by SEM and LM evaluations. The unirradiated left cornea appears to serve as an appropriate control. This damage appears to increase (1) as the irradiation is modulated by pulsing at the same power. (2) Damage increases as the same total energy is delivered ove

(continued on next page)

14. SUBJECT TERMS	15. NUMBER OF PAGES
Millimeter irradiation, cornea, accidental exposure safety, damage threshold, specific absorption rate	51
	16. PRICE CODE

17. SECURITY CLASSIFICATION OF REPORT	18. SECURITY CLASSIFICATION OF THIS PAGE	19. SECURITY CLASSIFICATION OF ABSTRACT	20. LIMITATION OF ABSTRA
Unclassified	Unclassified	Unclassified	Unlimited

a short period (15 min vs 0.2 sec), perhaps as a result of higher temperature values attained. (3) the lowest dose rate at which damage has been detected in preliminary experiments is 0.03 W/cm^2 (SAR 33 mWg) for pulsed irradiation for 15 min exposure. The threshold value implicit in the results above is below the safety threshold, when the safety factor of 10 is taken into account. (4) The threshold for CW irradiation at which damage was just discernable in 2 of 4 rabbits exposed was 0.5 W/cm^2 (SAR 550 mW/g).These experiments should be continued to permit further data to be gathered, since the threshold value implicit in the results above is rather close to the safety threshold, when the safety factor of 10 is taken into account.

To simulate an accidental exposure to a high power beam of millimeter waves, pulsed irradiation was delivered in 158 pulses of 20 KW peak power, 20 μseconds in length. This dose was just sufficient to cause damage over 15 minutes at a total dose of 69.3 J/g. Reducing the period of delivery of the 158 pulses to 0.2 sec (SAR 385 W/g) resulted in an enhancement of the damage. Associated with this was a temperature increase to no more than 44° C. Damage occurred in an oval area, and in several point areas of damage at pits in adjacent areas and peculiar traces. An endothelial bulge indicated the focal damage caused by the millimeter wave beam, which weakened the cornea. Massive disorganization of the corneal stroma was observed in the damaged area, and the oval weakened area in the SEM was susceptible to pressure from the electron beam, which caused a dimple in the endothelial surface. The amounts of damage observed similarly in two rabbits suggests that further test need to be performed to better define the damage threshold for short bursts of millimeter wave pulses.

FOREWORD

A. List of professional Personnel Employed on This Project

Principal Investigator	Dr. John R. Trevithick, Ph.D.
Research Consultant	Dr. Margaret O. Creighton, Ph.D.
	Dr. Maurice Hirst, Ph.D.
	Dr. A.P. Cullen, Ph.D.
	Dr. S.E. Sanford, D.V.M., Diploma of Vet. Pathol.
Research Associate	Dr. Madhu Sanwal, Ph.D.
Technical	Mr. T. Dzialoszynski

B. Animal Care

In conducting the research described in this report, the investigator(s) adhered to the "Guide for the Care and Use of Laboratory Animals" prepared by the Committee on Care and Use of Laboratory Animals of the Institute of Laboratory Animal Resources, National Research Council (DHEW Publication No. (NIH) 86-23; Revised 1985).

TABLE OF CONTENTS

PAGE

INTRODUCTION

Although millimeter wave radars are now strategically important, only one study of the effect of millimeter waves on the cornea has been reported (Rosenthal et al., 1975). This study did not use the pulsed mode of millimeter waves which is commonly in use in such radars. Because we have discovered apparent differences between similar doses of pulsed and CW microwaves (Stewart-DeHaan et al., 1980) in preliminary experiments and because we have succeeded in separating the effect of heating from the effects due to the electromagnetic field, for microwave cataract, we wished to devise a similar system for irradiation of the cornea *in vitro* which would offer similar advantages for the study of millimeter wave damage to the cornea.

The first step in these experiments was to devise appropriate media and conditions for the tissue culture of corneas, to be used for the experiments investigating their exposure to millimeter waves. The second step, also described in our Annual Report, June 1981 under DAMD17-80-G-9480, was to incubate the cultured corneas at different elevated temperatures in order to investigate the effect of incubation at elevated temperature on the cornea. The third stage, reported in our Annual Report, June 1982 under DAMD17-80-G-9480 and DAMD17-82-C-2018, was to test the effect of exposing incubated corneas to non-ionizing radiation, for which we selected ultraviolet as convenient and accessible in our laboratory, since the appropriate millimeter wave irradiation apparatus was not yet operating. In 1983 the millimeter wave irradiation apparatus was functioning, permitting us to form preliminary experiments on rabbits *in vivo* which were reported in the annual report (June 1983) for DAMD17-82-C-2018.

In the interim period Kues and his collaborators have reported deleterious effects of 2.45 GHz microwaves (Kues et al., 1985) in which for pulsed irradiation, a lower exposure level was necessary to induce equivalent damage when compared to CW irradiation. The incident irradiation levels these investigators used were at 10 mW/cm^2 or more, with a total power input of approximately 2.9 W with 50-150 mW reflected for the 10 mW/cm^2 condition, but the SAR was not determined. A latency period of approximately 1 day was required for the effects to appear, and the effects did not appear to be thermally caused, since only minimal temperature elevations occurred.

The experiments reported here, several of which were reported in our 1987 year end report, use several novel concepts to permit further information to be obtained regarding MM wave effects.

1. A focusing antenna permits a pencil beam of millimeter waves to be delivered to the target.
2. Since target and antenna are physically separated, applicator effects are avoided.
3. The surface temperature at any point on the target may be monitored continuously and recorded at intervals as small as 0.1 sec using the AGA thermovision computerized camera.

4. A computerized pachometry apparatus permits accurate records of corneal thickness to be obtained before and after irradiation at various times.
5. Photographic recording of corneal appearance by slit-lamp biomicroscopy, and retro-illumination photography of the cornea is combined with real-time video recording of the corneal appearance during irradiation by millimeter waves.
6. Development of a defined protocol for division of the cornea into areas to be used for SEM, LM, and TEM, and a defined procedure for examination of the divided areas by SEM and LM (and TEM as appropriate).
7. Quantification of the damage using a Zeiss videoplan to obtain a statistically valid measure of the millimeter-wave-induced damage.
8. Fluorescein staining of the cornea to visualize the de-epithelialization of areas or the cornea injured after exposure to the millimeter wave irradiation.

MATERIALS AND METHODS

Outline of Experimental Details

Animal Handling

New Zealand white rabbits were used in this study, housed in part at the University of Western Ontario Animal Quarters and at the Walter Reed Army Institute of Research (WRAIR). For *in vivo* irradiation at the WRAIR, rabbits were anesthetized using ketamine - rompun (xylazine) prior to and during irradiation of their corneas (see details below). Corneal temperature was monitored using a thermographic camera and when desired maintained by a current of moist air across the corneal surface. Irradiation was performed as described below. Following irradiation *in vivo*, after an appropriate period of latency, rabbits were reanesthetized (see details) for slit lamp and pachometry examination. Analgesia was provided as necessary to alleviate discomfort. At the end of the experiment, rabbits were killed by euthanasia with pentobarbitol, 230 mg/kg. The eyes were removed and the corneas dissected out, being careful not to damage the epithelium and endothelium - this was checked by scrutinizing each under a dissecting microscope.

Anesthesia

Rabbits were anesthetized by 30-50 mg/kg ketamine with Rompun (5-10 mg/Kg) injected intramuscularly. This does not have the side effect of lowering animal body temperature.

Materials and Methods

The anesthesia conditions were tested at the University of Western Ontario. Pulsed millimeter wave exposures took place at the WRAIR millimeter wave exposure chamber in Building 40. All exposures were at a frequency of 35 GHz. The exposure conditions used (Table 1) explored duration, peak power and total dose required for perceptible damage, as well as latency, in a preliminary way.

In vivo Irradiation

New Zealand white male rabbits, average weight 2.5 kg were irradiated using a special focusing antenna in a special rabbit carrier constructed of plexiglass and nylon parts which maintained their heads in a fixed position (Fig. 1) during the 15 min period of irradiation. The carrier was fastened to a large block of styrofoam by strong plastic lacing so that the optical axis of the rabbit's eye approximately coincided with the axis of the focusing antenna emitting the millimeter waves. The distance from the cornea to the front of the antenna was measured. For SAR determination the rabbit's corneal surface temperature was measured by recording the temperature reading of a thermographic camera (AGA Thermovision), see below.

RESULTS AND DISCUSSION

These results represent the first irradiation at 35 GHz which did not involve a contact applicator, and thus do not suffer from possible heating artefacts associated with contact applicators used in previous experiments. The cornea would experience similar effects when exposed to an outdoor millimeter wave radar transmitter source (i.e. surface absorption only). In order that the damage which occurs can be documented, it was necessary to devise methods for the following:

1. Slit lamp biomicroscopic examination of the rabbits and photographic recording of the results.
2. Anesthesia.
3. Measurement of temperature of cornea using thermographic camera and calculation of SAR (specific absorption rate) during irradiation by 35 GHz waves.
4. Cooling of corneas by air cooling (exploration of feasibility).
5. Computerized recording by pachometry of thickness of cornea.
6. Reproducible dissection and fixation of corneas.
7. Division of cornea into sections for examination by SEM, LM and TEM.
8. Reproducible examination of samples.
9. Classification of types of damage.
10. Quantification of damage using Zeiss videoplan.

1. Slit Lamp Biomicroscopy

We have used this technique to observe changes between the appearance, by Zeiss-slit lamp biomicroscope of the cornea before and after irradiation, by retro-illumination, and slit-lamp illumination, both coupled with photography and pachometry using a computerized apparatus to quantify changes in corneal thickness.

2. Anesthesia

Experiments with anesthesia of the rabbits revealed that the corneal reflex was abolished reproducibly for the period between 10 and 25 min. from the initial injection using ketamine (35 mg/kg) and xylazine (5 mg/kg). The reflex returned slowly towards normal, which was attained after 60 min from the initial injection.

3. Measurement of Corneal Temperature with Thermographic Camera

Figure 1 illustrates the rabbit head in holder and its imaging (Fig. 2) by photography (a), thermography (b) and thermographic profile (c). The temperature of the cornea was measured using an AGA thermovision 780 system equipped with a BMC computer analysis system programmed using the disco 2.0.1 system (Gesotec, Federal Republic of Germany), for image recording and analysis. The range of corneal temperatures (Fig. 3) observed was 19.5-32°C. A relatively flat oblong plateau at the maximum temperature (32° C) occupied the central area of the cornea rising steeply from the lower temperature at the bottom and the top of the eye.

Phantom SAR studies for millimeter wave irradiation

(a) spot size: Thermographic images of the temperature distribution immediately before and after millimeter wave irradiation of the corneal phantom were analyzed as an oblong rounded spot within the center of the phantom. Here the most significant surface temperature elevation occurred (Fig. 4). Computer image-processing was used to analyse the thermographic subtraction image (including vertical and horizontal linear-scan profiles) that was obtained following subtraction of initial from final temperatures found on exposure to the millimeter wave irradiation. The vertical and horizontal scan-line profiles that passed through the center of the spot indicated smooth curves with no apparent hot spots or sharp increases in temperature within the spot (Fig. 5a, b). The spot size of the region that experienced a measurable temperature rise during irradiation was defined by using the width of the area where the temperature rise was one half of the maximum value of the peak temperature rise. The absolute distance across the corneal surface was estimated by calibrating the thermographic camera's spatial display with a heated metal reference object. This rectangular object was imaged at the same camera-to-subject distance as the camera-to-cornea distance that was used during the millimeter wave SAR experiments. Using this approach, the horizontal widths of the millimeter-wave heat spot on the phantom were found to be 0.7 cm (Fig. 5a) when the phantom was surface positioned at the focal point of the transmitting antenna. When the phantom surface was placed at distances of 2.5 cm (Fig. 5d) and 5 cm from the antenna's focal point, farther along the axis of propagation the horizontal widths of the heated spot were 1.25 cm and 2.3 cm (not shown) respectively. The vertical heights of the heated spots were 1.09 cm (Fig 5b) at the antenna focal point, 1.35 cm (not shown) for an antenna-to-phantom distance that was 2.5 cm farther from the focal point, and 2.8 cm when the separation distance was increased to a distance that was 5 cm from the focal point. A similar sized spot was estimated for the rabbit eye (Fig. 6,7).

Peak SAR values for cornea and phantom

The peak SAR was estimated using the maximum temperature elevation at the peak of the temperature plot. The calculation of the SAR utilized the following approximations for the value of the specific heat of the irradiated objects. Since the tissue of the cornea and the cucumber have a very high water content, the specific heat and mass density of water were used. Using this approximation, the spatial peak SAR values calculated for the phantom, (obtained for an average radiated power of 4W) were 1.1 W/kg per Watt of average transmitted power, or 1.46 ± 0.3 mW/g per mW/sq cm of radiated power. For the rabbits, an average radiated power of 0.38 W was used to obtain an SAR value 1.1 W/kg per Watt of average transmitted power, or 1.43 ± 0.34 mw/g per mW/sq cm of radiated power. These results indicate that the SAR of the cornea of the rabbit and in the phantom (cucumber) are nominally identical. For this reason, it appears that use of a cucumber as phantom was a useful and practical alternative to the sacrifice of rabbits. This is especially true for the preliminary experiments involving the determination of the optimum location of the subject being irradiated, and for the determination of corneal SAR (magnitude and spatial distribution). Also, the use of the phantom offered advantages of (1) not requiring animals subjected to anesthesia and (2)

permitting effects of higher average powers (4w) to be tested without air cooling. This, in turn, enabled higher signal to noise ratios to be obtained during the acquisition of thermographic data.

4. Corneal Cooling by Air Flow

Air flow from a Fisher vacuum/pressure medical pump through a gas-washing bottle containing water equilibrated the air with water vapour, so that at the temperature of released air (20°C approximately) blowing on the rabbit eye, the relative humidity of the air was 80% or greater. Several air flow rates were used, resulting in differential cooling. At a particular flow rate (10 psi pressure at pump corresponding to 16.9 1/min air flow), the corneal peak temperature elevation was a linear function of the incident power. When the air flow rate was increased with no heating, the temperature decreased linearly with increased flow rate (Fig. 8).

Influence of power applied and air flow on corneal heating

Millimeter wave heating by continuous wave irradiation was studied in the absence of air flow. Increasing the power applied resulted in an increase in temperature of the hottest point on the corneal surface, which was a linear function of the applied power (Fig. 9), within the range of power up to 2 W average power. The addition of air cooling resulted in a lower increase in temperature for a given level of radiated power used for heating the cornea. This seemed to agree with the earlier findings from the corneal cooling experiments that were performed in the absence of millimeter wave irradiation. As the air flow rate was increased for a constant radiated power level, the amount of temperature rise decreased with higher air flow rates resulting in the observation that the temperature elevation with no air flow at 0.75 W/sq cm was identical to that with 34 1/min air flow at 2.25 W/sq cm. thus 34 1/min apparently provides cooling equivalent to 1.5 W/sq cm.

5. Computerized Pachometry Measurement of Corneal Thickness

Dr. A. Cullen has arranged for computerized operation of a Zeiss pachometer he has modified electronically, when activated by a foot switch, to record the reading and average 7 or 8 successive readings to give a result for each of average ±SE. It was possible to estimate differences between corneal thickness, before and after exposure, to an accuracy of 1 μm. In later experiments no increase between initial and final thickness occurred as a function of microwave irradiation. For this reason it was decided only to use this technique for experiments involving latency which afford an opportunity for corneal swelling to occur.

6. Fixation of Corneas

The corneal epithelium was pre-fixed in situ with two drops of Karnovsky's fixative immediately following euthanasia of the rabbit. After a 2-3 min. pre-fixation period, the cornea was cut off with a rim of sclera. After making a nick to identify the nasal area, it

and the other portions of the eye were fixed with gentle agitation in Karnovsky's fixative at 4° C for 24-48 hr then transferred to 0.1 M sodium cacodylate buffer, pH 7.2.

7. Division of Corneas for Examination by SEM, LM and TEM

Figure 10 shows the diagram of dissection of the corneas into segments for examination by Scanning Electron Microscopy (SEM), light microscopy (LM) and Transmission Electron Microscopy (TEM). The center strips are removed (see below) and opposing segments (1 & 3 or 2 & 4) are placed together in a small vial containing fixative or cacodylate buffer. Where appropriate the sections 1 & 3 were used to view epithelial surfaces, the sections 2 & 4 to view endothelial surfaces. The sections were processed in the usual manner for SEM (dehydration through alcohol series and critical point drying, then afterwards attached to aluminum stubs with either silver daube paint or nickel paint, and spattered with gold palladium). The 2 mm wide strip taken at the equatorial zone was put away as sample C. The nasal area was marked by a diagonal cut. After both anterior and posterior halves of the cornea were bisected, 2 mm strips were taken from the middle and labelled A and B. As before, a diagonal cut was made at the central area. A, B, C were processed as appropriate for LM and TEM. They were postfixed in 1% osmic acid for 2 hours, washed, dehydrated and prepared for embedding in Epon or Spurr resin. After the final stage of resin infiltration, the long strips of cornea were placed on a piece of dental wax and cut in 1.5 mm blocks by a sharp blade. The cut pieces of tissue were embedded in numbered flat embedding modules; # 1 being the diagonally cut end. This enabled the location of the exact position of any block being studied to be determined. Generally, semithin sections were cut where appropriate from alternate numbered blocks, stained with toluidine blue and viewed under LM for general morphology, and pertinent areas photographed. Some representative areas were selected and ultrathin sections were cut to be studied later (not done) under TEM after staining with uranyl acetate and lead citrate.

8. Reproducible Examination of Samples

a) By SEM: The corneas, dissected as illustrated in Fig. 10, were viewed systematically on the stub; three viewing lines were established, at 500 m, 1000 m and 2000 m from the sclera (See Fig. 10 cutting diagram) - both epithelial and endothelial surfaces. Initially each specimen was scanned completely along these lines and 3 pictures taken at three randomly choosen spots on this line as 100X, 500X, 1000X, 5000X as indicated by Dr. Michael Doughty. At 100X the percent of the area occupied by lesions could be assessed; at 500X the light cells vs the dark cells could be compared; at 1000X the state of the cell border could be noted. However, such extensive photography was very expensive. It was therefore decided to take one picture at each of the 3 viewing lines at 500X for epithelial and 1000X for endothelial, after a visual inspection and conscious decision to photograph one specific area, as typical of the cell's condition at that view line. The pictures thus obtained were evaluated using a computerized Zeiss videoplan which gives individual cell areas, mean cell area and standard deviation, as well as cell perimeters. Using this method, areas of normal and abnormal cells for each rabbit cornea could be found and corneal comparisons made.

b) LM and TEM Thick and/Thin Sections

9. **Types of Damage Found**

a) Irradiation conditions: It will be noted that most early (low in the numerical order) trials had moist air flow over the cornea and that the rabbit was sacrificed immediately. However, immediately sacrificed animals, which were the last rabbits done in June 1986 (ie: #48-52) had no air cooling since it was found in experiments analysed by this time that the moist airflow was damaging the cornea.

It should be noted that rabbits 1-6 are composite experiments being given different sequential doses over 15 mins. Some information as to their final handling was lacking in the original notes.

b) SEM: (i) Visual library: During the assessment of the rabbit corneas examples of various degrees of damage were photographed and a simple system of nomenclature given to indicate degree of damage. N = Normal, Type I (a) - single cells missing, appear lifted whole from surface leaving "cooked" or coagulated area where cell was (Fig. 11); (b) numerous cells missing - like to Type Ia (Fig. 11a); (c) areas of single cells running together, like to Type Ia (Fig. 11b); (c) areas of single cells running together, like to Type Ia (Fig. 11b). Type II, similar to Type I but area more extensive a-c (Fig. 11c). Type III: whole area of 500X photo is damaged (Fig. 11d).

(ii) Videoplan assessment of percent damage as a function of area: This shows the percentage of epithelial cells damaged as compared to the total number of cells visualized at a constant magnification of 500X at the various predetermined lines (500 m, 1000 m, 2000 m from the sclera towards the center of the cornea) on the corneal surface. It would appear that except for certain exceptions (rabbit #3, rabbit #49) the unexposed left cornea acted as a good control to the experiment.

(iii) Comparison of Pu-CW irradiation and pulse-power and time combinations: The accompanying Table 1 shows the samples from comparable exposure conditions at similar total input energy.

c) Light microscopy of thick plastic sections: Light microscopy revealed several types of damage, presented in order of increasing amount: Type L1 (Fig. 12a) outer epithelial cells lifting off as shown by arrow; Type L2 (Fig. 12b) in addition to lifting cells, the outer epithelial cells have groups of darkly stained cells which are apparently heavily damaged and thus degenerating; Type L3 larger areas of cornea (Fig. 12c) with more severe cell loss including complete loss of epithelial cells in some areas with exposure of the stomal surface; Type L4, light staining in the upper layers is consistent with cell death, while lower epithelial cells are more darkly staining, indicating severe damage (Fig. 13).

(d) Pu, CW Thresholds : See Table 2:

(1) the damage observed using pulsed irradiation appears to be greater than for CW at similar average powers. (2) The lowest average power investigated produced a

significant damage for pulsed irradiation. This was at 0.03 W incident power (spatial peak SAR 33 mW/g temporal). This value expressed as power density over a 1.3 cm diameter spot is approximately 0.3/1.327 cm^2 = 0.0226 mW/cm^2 which is only a factor of 4 above the safety limits suggested for whole body irradiation at this wavelength and also a factor of 4 above the local SAR ("partial body exposure") safety limits. (3) The finding that damage appeared more extensive for pulsed (modulated) than CW irradiation at similar average powers suggested that our previous findings of more damage from pulsed than CW irradiation also is true at 35 GHz as well as at 0.918 GHz. More work is required to accurately quantify the factor by which the damage is increased because of modulation of the irradiation, and to explore the effect of pulse parameters, exposure duration, average power, temperature elevation and air cooling on the effect observed. Further work is needed to investigate the effect of lower powers on corneal damage, to determine whether significant damage occurs at lower power levels, and whether the threshold is different for pulsed as compared to CW irradiation.

Comparison of total dose in Joules between our work and that of Kues et al. (1985) reveals a striking similarity between conditions he found damaging for pulsed microwaves (150 J/kg) and our exposures 29.7 J/kg at the minimum level at which detectable damage was found.

(e) Pu Accidental Exposure: Figures 14-16:

Thermographic imaging indicated a maximum increase in temperature in the irradiated area of 9.5°C in rabbit 118, irradiated for 0.18 seconds (Figure 14) , from the normal rabbit corneal temperature of approximately 34.5°C. Severe damage was caused by the 0.18 sec exposure to 158 pulses of 20 μsec, at a spatial peak SAR of 22 kW/g.

At this duration and dose rate, each of 2 rabbits (#117, 118) vocalized, moved their heads and closed the irradiated eye after irradiation (on video recording, not shown here). Thermographic imaging indicated an increased temperature, to no more than 44° C, from the normal corneal temperature of 34.5° C. In other experiments at lower dose rates which achieved the same or higher corneal surface temperatures, i.e. rabbits 13 (14.3°C), 16 (11.8°C), 43 (10°C) no similar response was observed, nor was the corneal damage observed as great.

In the irradiated area, damage observed by scanning microscopy occurred in an oval area positioned across the border between quadrant 1 and 4, with the border equally dividing the oval damaged area along its short axis. (Fig. 15A-D) At the endothelial surface an unusual bulge in the endothelial cellular sheet may indicate the force or pressure which was exerted by the exposure to the pulsed millimeter wave beam. That this is a bona fide bulge was shown by its behaviour on exposure to the electron beam in the scanning microscope, which produced a dimple in the bulge (Fig. 16).

By light microscopy of thick plastic sections in the oval area no epithelial cells were seen covering the oval area, (Fig. 17A-E) while at the borders of the area finger-like projections of the corneal stroma covered with one layer of epithelial cells instead of the usually multilayered structure of the epithelium. The stroma has apparently been disrupted so that it appears to have flowed or snapped back, like a rubber band suddenly released

from tension, to form the underlying support of these cells, while retaining its layered structure (Fig. 17E).

CONCLUSIONS

This study has been an introductory survey of corneal effects of pulsed (Pu), 35 GHz millimeter waves and a comparison with damage by continuous wave (CW) at similar average powers and defined specific absorption rate (SAR) values. Based on these results it is recommended that animal handling be minimized and air flow be 5 psi or lower. Use of the left cornea (unirradiated) as control seems to be appropriate providing no damage occurs during animal handling.

Several findings, although they require further confirmation, should be noted as potentially important for safety standard revisions which may eventually be contemplated by regulatory authorities:

(1) the damage observed using pulsed irradiation appears to be greater than for CW at similar average powers.

(2) the damage appears to increase as the irradiation is modulated by pulsing at the same average power.

(3) The threshold for CW irradiation at which damage was just discernable in 2 of 4 rabbits exposed was 0.5 W/cm^2 (SAR 550 mW/g).

(4) the lowest dose rate at which damage has been detected in preliminary experiments is 0.03 W/cm^2 (SAR 33 mW/g) for pulsed irradiation for 15 min exposure. The threshold value implicit in the results above is below the safety threshold, when the usual safety factor of 10 is taken into account:

The lowest average power investigated, which produced significant damage for pulsed irradiation, was 0.03 W incident power (spatial peak SAR 33 mW/g temporal). This value expressed as power density over a 1.3 cm diameter spot is approximately 0.3/1.327 cm^2 = 0.0226 mW/cm^2 which is only a factor of 4 above safety limits suggested for whole body irradiation at this wavelength and also a factor of 4 above the local SAR ("partial body exposure") safety limits.

(5) The finding that damage appeared more extensive for pulsed (modulated) than CW irradiation at similar average powers suggested that our previous findings of more damage from pulsed than CW irradiation also is true at 35 GHz as well as at 0.918 GHz. More work is required to accurately quantify the factor by which the damage is increased because of modulation of the irradiation, and to explore the effect of pulse parameters, exposure duration, average power, temperature elevation and air cooling on the effect observed. Further work is needed to investigate the effect of lower powers on corneal damage, to determine whether significant damage occurs at lower power levels, and

whether the threshold is different for pulsed as compared to CW irradiation.

(6) Comparison of total dose in Joules between our work and that of Kues et al. (1985) reveals a striking similarity between conditions he found damaging for pulsed microwaves (150 J/kg) and our exposures 54 J/kg at the minimum level at which detectable damage was found.

(7) Although modelling (158 pulses) at approximately twice the threshold dose over a 9 second period was expected to result in a similar temperature elevation (9.5°C), much less damage was observed for this period of irradiation. The damage observed when the same dose was delivered over approximately 0.18 seconds, which would be expected to result in about the same temperature increase, was significantly increased, as was the biological effect, causing the animal even in stage 4 anesthesia to jump, close its eye and vocalize to avoid the discomfort elicited by the series of pulses.

What could account for this difference in extent of damage and the nervous system overcoming stage 4 anesthesia? Physiologists with whom we have consulted indicate that the steepness of the slope of the temperature increase curve could have triggered a reflex response resulting in the involuntary jerk of the rabbit head, just as a rapid reflex response to a burn on a finger in a human causes us to involuntarily jerk away because of the rapid temperature increase. A similar reflex eye closing, jumping and vocalizing in deep anesthesia has been reported, in response to the intraocular injection or topical application to the cornea of capsaicin, the active principle of red peppers (Camras and Bito, 1980). The reflex-stimulating injection was previously attributed to depletion of Substance P in nerve endings (Jessell, Iverson and Cuello, 1978).

The effect of destruction of the corneal epithelium and the associated thermoelastic transduction-induced pressure wave are very reminiscent of the ablation of corneal tissue occurring in the now common operation to correct vision using excimer laser. In the latter case, each excimer laser pulse also generates a pressure shock wave during the ablation of the corneal tissue, by the same process of thermoelastic transduction of energy, and as well causes localized heating of the corneal epithelium and stroma.

This result suggests that it may be important to consider the actual duration of the exposure to pulsed millimeter radiation, since shortening the period over which the exposure is delivered may increase the damage even though the total energy delivered and the temperature elevation attained do not differ from longer durations of exposure.

Summary of Overall Conclusions from These Experiments

1. The higher the wattage the greater the damage to the cornea.
2. At higher wattages the damage area seems confirmed to the central region at which the millimeter waves are targeted.
3. Millimeter waves modulated by pulsing seem to be more damaging than CW at similar average powers.

4. Handling of the animals should be kept at a minimum as damage results easily.
5. The left cornea can be used as a control but there may be background damage due to handling which must be taken into account.
6. The threshold exposure for 15 minute exposures occurs at a value of the SAR of 550 mW/g for continuous wave millimeter waves, and at a much lower value for pulsed millimeter waves, 33 mW/g, a factor of approximately 15 fold difference between the two modes.
7. The modelling of accidental exposure to millimeter waves indicates that the period over which the pulses are delivered may play a critical role, even though the temperature increase to 44.5°C is less than 10°C above the normal corneal temperature, a temperature which it is possible to encounter in terrestrial environments such as the heat waves occurring in India and Pakistan in the summer of 1995.

REFERENCES

Camras, C.B. and Bito, L.Z. (1980). "The pathophysiological effects of nitrogen mustard on the rabbit eye. II. The inhibition of the initial hypertensive phase by capsaicin and the apparent role of substance P". Inv. Opthalmol. Visual Sci. 19:423-438.

Carpenter, R.L., Van Ummersen, C.A. (1968). J. Microwave Power 3:3-19.

Carpenter, R.L., Ferri, E.S., Hagan, G.L. (1974). Proc. Int. Symp. Biologic Effects Health Hazard Microwave Radiation (Warsaw), pp. 178-184.

Durney, C.H., Iskander, M.F., Massoudi, H., Allen, S.J., Mitchell, J.C. (1980). "Radiofrequency Radiation Dosimetry Handbook." Report SAM-TR-80-32, pp. 28-29.

Dyer, F.B. (1981). MM Wave Innovation: The Challenge in the EW Community Military Electronics/Countermeasures, pp. 84-90.

Jessell, F.M., Iversen, L.L. and Cuello, A.C. (1978). "Capsaicin-induced depletion of Substance P from primary sensory neurones. Brain Res. 152:183.

Kues, H.A., Hirst, L.W., Lutty, G.A., d'Anna, S.A. and Dunkelberger, G.R. (1985). Bioelectromagnetics 6:177-183.

Mousa, G.Y. and Trevithick, J.R. (1977). Developmental Biol. 60:14-25.

Ready, E.K. (1980). Millimeter Radar-fundamentals and Applications. Military Electronics/Countermeasures August (Part One) and September (Part Two).

Rosenthal, S.W., Burenbaum, L., Kaplan, I.T., Methlay, W., Synder, W.E. and Zaret, M.M. (1975). Proc. USNC/URSI Annual Meeting (Boulder, CO) 1:110-128.

Rosenthal, S.W., Burenbaum, L., Kaplan, I.T., Methlay, W., Synder, W.E. and Zaret, M.M. (1975). In Biological Effect of electromagnetic waves, vol. I. Johnson, C.C. and Shore, M.L. Editors, HEW Publication (FDA) 77-8010.

Spentz, D.J., Peyman, G.A. (1976). Invest. Ophthalmol. Vis. Sci. 15:1000-1002.

Stewart-DeHaan, P.J., Creighton, M.O., Larsen, L.E., Jacobi, J.H., Ross, W.M. and Trevithick, J.R. (1980). IEEE MTT-S International Microwave Symposium Digest Institute of Electrical and Electronics Engineers. Piscataway, N.J., pp. 341-345.

Van Horn, D.L., Hyndiuk, R.A. (1975). Exp. Eye Res. 21:113-124.

APPENDIX

TABLE 1 (see notes)

Rabbit Number	Air	Time/W Time x Av. Power	E(tot) Joules/ kg	Peak Pow W	PW μS	Peak SAR Kw/Kg	E/pulse J	AvSAR W/kg	ΔT°C	Damage/	%
1		40 sec x 5.65 W	249	23kW	20 μS	25.3	0.46	6.22	9	N.D.	
2		40 sec x 4.5 W	198	23kW	20 μS	25.3	0.46	4.95		N.D.	13%
3		40 sec x 4.95 W	219.8	23kW	20 μS	25.3	0.46	4.90	4.3	N.D.	14%
4		40 sec x 4.5 W	198	23kW	20 μS	25.3	0.46	4.95	6.9	N.D.	10%
5		40 sec x 4.43 W	195	23kW	20 μS	25.3	0.46	4.9	4.5	N.D.	34%
6		40 sec x 7.9 W	348	23kW	20 μS	25.3	0.46	8.69	4.7	N.D.	0
7		15 min x .5 W	495	24kW	2 μS	26.4	0.048	0.55	3.0	N.D.	16.5%
8		15 min x 1 W	990	24kW	2 μS	26.4	0.048	1.1	3.0	N.D.	18%
9			0	24kW	2 μS	26.4	0.048	-	-	N.D.	N.D.
10		15 min x .5 W	495	24kW	2 μS	26.4	0.048	.55	3.6	N.D.	N.D.
11		15 min x 1.9 W	1881	24kW	2 μS	26.4	0.048	2.09	5.5	N.D.	N.D.
12		15 min x 2.0 W	1980	24kW	2 μS	26.4	0.048	2.2	8.5	N.D.	N.D.
13		15 min x 1.5 W	1485	24KW	2 μS	26.4	0.048	1.65	14.3	N.D.	N.D.
14		15 min x 0 W	0	-	-	-	-	-	10.2	N.D.	N.D.
15		7.5 min x 3.0 W	1485	20kW	2 μS	22	.04	3.3	15.8	N.D.	N.D.
16		10.5 min x 3.0 W	1040	22kw	2 μS	24.2	.044	3.3	11.4	N.D.	N.D.

Rabbit Number	Air	Time/W Time x Av. Power	E(tot) Joules/kg	Peak Pow W	PW μS	Peak SAR Kw/Kg	E/pulse J	AvSAR W/kg	ΔT°C	Damage/	%
17	Air	15 min x 3.0 W	1	22kW	2 μS	24.2	0.044		9.0	N.D.	N.D.
18	A	15 min x 0 W	0	SH	SH	-	-		-	N.D.	N.D.
19	?	15 min x 2 W	1980	22kW	2 μS	24.2	0.044		-3	N.D.	N.D.
20	?	15 min x 2 W	1980	22kW	2 μS	24.2	0.044		3.1	N.D.	N.D.
21	A10	15 min x 1 W	990	24kW	2 μS	26.4	0.044		5.0	N.D.	N.D.
22	-	15 min x 1 W	990	24kW	2 μS	26.4	0.044		7.0	N.D.	N.D.
23	-	15 min x 0.5 W	495	24kW	2 μS	26.4	0.044		0.9	N.D.	N.D.
24	A	15 min x 0.5 W	495	24kW	2 μS	26.4	0.044		-3.6	N.D.	N.D.
25	A20	15 min x 3.0 W	2970	20kW	20 μS	22	0.4		3.5	N.D.	N.D.
26	A10	15 min x 3.0 W	2970	20kW	20 μS	22	0.44			N.D.	N.D.
27	A20	5 min x 3.0 W	990	20kW	20 μS	22	0.44		5.8	N.D.	N.D.
28	A10	1.5 min x 3.0 W	297	20kW	20 μS	22	0.44		1.7	N.D.	N.D.
29	A10	5 min x 1.0 W	330	20kW	20 μS	22	0.44		1.7	N.D.	N.D.
30	A10	1.5 min x 1.0 W	99	20kW	20 μS	22	0.44		-3	N.D.	N.D.
31	A10	15 min x 0.3 W	29.7	20kW	20 μS	22	0.44			N.D.	N.D.
32	A10	.5 min x 0.3 W	9.9	20kW	20 μS	22	0.44		-1.8	N.D.	N.D.

Rabbit Number	Air	Time/W Time x Av. Power	E(tot) Joules/kg	Peak Pow W	PW μS	Peak SAR Kw/Kg	E/pulse J	AvSAR W/kg	ΔT°C	Damage/	%
33	A10	1.5 min x 0.3 W	29.7	20kW	20 μS	22	0.44			N.D.	N.D.
34	A10	15 min x 0.1 W	99	20kW	20 μS	22	0.44		7.0	N.D.	N.D.
35	A10	5 min x 0 W	0	SH	SH	SH	-		0	N.D.	N.D.
36	A20	20 sec x 10 W	220	20kW	20 μS	22	0.44	11		N.D.	9.2%
Blink 37	A20	0.95 sec 100 W	1045	20kW	20 μS	22	0.44	11	14	N.D.	N.D.
38	A20	0.15 sec 300 W	49.5	20kW	20 μS	22	0.44	11	0	N.D.	N.D.
39	A20	0.2 sec 300 W	66	20kW	20 μS	22	0.44	11	8.1	N.D.	N.D.
40	A20	0.2 sec 450 W	99	20kW	20 μS	22	0.44	11		N.D.	N.D.
41	A20	1.5 min x 0	0	SH	SH	SH	SH	-	-4.8	N.D.	N.D.
42	A10	.1 sec 100 W	11	20kW	20 μS	22	0.4	-	1.2	N.D.	N.D.
43	A10	.2 sec 450 W	99	20kW	20 μS	22	0.4	495	10.0	N.D.	34%
44	A10	5 min x 0.1 W	33	20kW	20 μS		0.44	495	-0.5	N.D.	N.D.
45	A10	1.5 min x 0.1 W	9.9	20kW	20 μS		0.44	495	0.3	N.D.	N.D.
46	A0	0.5 min SH	0	SH	SH	SH	SH	-	0	N.D.	N.D.
47	A10	15 min SH	0	SH	SH	SH	SH	-	0	N.D.	N.D.
48	-	-	-	-	-	-	-	-	-	N.D.	N.D.

Rabbit Number	Air	Time/W Time x Av. Power	E(tot) Joules/kg	Peak Pow W	PW μS	Peak SAR Kw/Kg	E/pulse J	AvSAR W/kg	ΔT°C	Damage/	%
49	A0	15 min x 0.03 W	29.7	20kW	20 μS	22	0.4	.033	0	N.D.	4.2%
50	A0	15 min x .03 W	29.7	20kW	20 μS	22	0.4	.033	0	N.D.	2.5%
51	A0	15 min x 0.03 W	29.7	20kW	20 μS	22	0.4	.033	0	N.D.	N.D.
52	A0	15 min x 0.03 W	29.7	20kW	20 μS	22	0.4	.033	0	N.D.	25%
53	A0	15 min SH	0	SH	SH	SH	SH	0	0	N	4.5%
54	A5 - 20	SH	0	SH	SH	SH	SH	0	0		
55	A5 - 20	SH	0	SH	SH	SH	SH	0	0	N-II	13.2%
56CW	A0	15 min x 0.5 W	495	CW	CW	CW	CW	0.55		N	1.5%
57CW	A10	15 min x 0.5 W	495	CW	CW	CW	-	0.55		I & II	14.6%
58CW	A5	15 min x 0.5 W	495	CW	CW	CW	-	0.55		N	5.1%
59CW	A5	15 min x 1.0 W	990	CW	CW	CW	-	1.1		N	3.4%
60CW	A0	15 min x 1.0 W	990	CW	CW	CW	-	1.1		I	12.4%
61CW	A0	15 min x 1.0 W	990	CW	CW	CW	-	0.11		I	6.2%
62CW	A0	15 min x 0.1 W	99	CW	CW	CW	-	0.11		N	4.3%
63CW	A0	15 min x 0.1 W	99	CW	CW	CW	-	0.044		N	5.1%
64CW	A0	15 min x 0.04 W	39.6	CW	CW	CW				X Bad	

Rabbit Number	Air	Time/W Time x Av. Pow er	E(tot) Joules/kg	Peak Pow W	PW μS	Peak SAR Kw/Kg	E/pulse J	AvSAR W/kg	ΔT°C	Damage/	%
65CW	A0	15 min x 0.04 W	39.6	CW	CW	22	-	0.044	3.0	X Bad	
66	A0	15 min SH	0				-	0	0.9	X Wrinkled	
67	A0	15 min x 0.5 W	495	20kW	20 μS	22	0.4	0.55	3.3	X	
68CW	A0	15 min x 0.5 W	495	CW	CW	CW	-	0.55	3.4	X	
69CW	A0	15 min x 1.0 W	990	CW	CW	CW	-	1.1	6.1	X	
70CW	A0	15 min x 1.0 W	990	CW	CW	CW	-	1.1	3.8	X	
71CW	A0	15 min x 1.0 W	990	CW	CW	CW	-	1.1	2.2	X	
72CW	A0	15 min x 0.5 W	495	CW	CW	CW	-	0.55	3.3	X	
73CW	A0	15 min x 0.5 W	495	CW	CW	CW	-	0.55	2.5	N	2.3%
74CW	A0	15 min x 0.5 W	495	CW	CW	CW	-	0.55	5.4	X	
75CW	A0	15 min x 1.0 W	990	CW	CW	CW	-	1.1	5.7	X	
76CW	A0	15 min x 0.04 W	39.6	CW	CW	CW	-	0.044		N	
77CW	A0	15 min x 0.1 W	99	CW	CW	CW	-	0.11		X	
78CW	A0	15 min x 0.5 W	495	CW	CW	CW	-	0.55		N	1.8%
79P	A0	15 min x 0.5 W	495	20kW	20 μS	22	0.4	0.55		X	
80P	A0	15 min x 0.04 W	39.6	20kW	20 μS	22		0.044		I	8.2%

Rabbit Number	Air	Time/W Time x Av. Power	E(tot) Joules/kg	Peak Pow W	PW μS	Peak SAR Kw/Kg	E/pulse J	AvSAR W/kg	ΔT°C	Damage/	%
81P	A0	15 min x 0.02 W	19.8	20kW	20 μS	22	0.44	0.044		N	3%
82P	A0	15 min x 0.03 W	29.7	20kW	20 μS	22	0.44	0.033		N	8.5%
83P	A0	15 min x 0.1 W	99	20kW	20 μS	22	0.44	0.11		Stain Damage	
84P	A0	15 min x 0.1 W	99	20kW	20 μS	22	0.44	0.11		X	
85P	A0	15 min x 0.5 W	495	20kW	20 μS	22	0.44	0.55		X	
86P	A0	15 min x 0.5 W	495	20kW	20 μS x1.25	22	0.44	0.55		X	
87P	A0	15 min x 0.1 W	99	20kW	20 μS x 225	22	0.44	0.11		X	
88P	A0	15 min x 0.1 W	99	20kW	20 μS	22	0.44	0.11		X	
89SL	A0	15 min SH	0	SH	SH	SH	SH	0		X	
90P	A0	15 min x 0.04 W	39.6	20kW	20 μS x 90	22	0.44	0.044		X	
91P	A0	15 min x 0.04 W	39.6	20kW	20 μS x 90	22	0.44	0.044		X	
92P	A0	15 min x 0.04 W	39.6	20kW	20 μS x 90	22	0.44	0.044		X	
93P	A0	15 min x 0.5 W	495	20kW	20 μS x 1125	22	0.44	0.55		X	
94P	A0	15 min x 0.5 W	495	20kW	20 μS x 1125	22	0.44	0.55		I-III	22%
95P	A0	15 min x 0.5 W	495	20kW	20 μS x 1125	22	0.44	0.55		I, II	17.4%
96P	A0	15 min x 0.10	99	20kW	20 μS x 1125	22	0.44	0.11		I-III	25.4%

Rabbit Number	Air	Time/W Time x Av. Power	E(tot) Joules/kg	Peak Pow W	PW μS	Peak SAR Kw/Kg	E/pulse J	AvSAR W/kg	ΔT °C	Damage/	%
97P	A0	15 min x 0.1 W	99	20kW	20 μS x 225	22	0.44	0.11		II	21%
98P	A0	15 min x 0.04 W	39.6	20kW	20 μS x 90	22	0.44	0.044		I	10.4%
99SL	A0	15 min SH	0	SH	SH	SH	SH	SH		N	4.6%
100P	A0	15 min x 0.04 W	39.6	20kW	20 μS x 90	22	0.44	0.044		N	4.3%
101	A0	15 min x 0.07 W	69.3	29kW	20 μS x 158	22	0.44	0.077		I-II	12.4%
102			-					-		X	
103			-					-		X	
104	A0	15 min x 0.07 W	69.3	20kW	20 μS x 158	22	0.44	0.077		I-II	10%
105	A0	15 min x 0.07 W	69.3	20kW	20 μS x 158	22	0.44	0.077	0.8	N	0
106	SH	15 min x SH	0	SH	SH	SH	-	SH	0	N	0
107	A0	15 min x 0.07 W	69.3	20kW	20 μS x 158	22	0.44	0.077	0	N	0
108	A0	15 min x 0.07 W	69.3	20kW	20 μS x 158	22	0.44	0.077	-	N	0
109	A0	15 min x 0.07 W	69.3	20kW	20 μS x 158	22	0.44	0.077	2.1	N	0
110	A0	15 min x 0.07 W	69.3	20kW	20 μS x 158	22	0.44	0.077	1.4	N	0
111	A0	1.5 min x 0.7 W	69.3	20kW	20 μS x 158	22	0.44	0.77	-	X	-

Rabbit Number	Air	Time/W Time x Av. Power	E(tot) Joules/kg	Peak Pow W	PW μS	Peak SAR Kw/Kg	E/pulse J	AvSAR W/kg	ΔT° C	Damage	%
112	A0	1.5 min x 0.7 W	69.3	20kW	20 μS x 158	22	0.44	0.77	-	-	-
113	A0	9 sec x 7.0 W	69.3	20kW	20 μS x 158	22	0.44	7.7	-	N	0
114	A0	9 sec x 7.0 W	69.3	20kW	20 μS x 158	22	0.44	7.7	-	II	
115	A0	9 sec x 7.0 W	69.3	20kW	20 μS x 158	22	0.44	7.7	-		
116	A0	5 min SH	0	-	-	SH	SH	SH	-	N	0
117	A0	0.18 sec x 350 W	69.3	20kW	20 μS x 158	22	0.44	385	-	III	
118	A0	0.18 sec x 350 W	69.3	20kW	20 μS x 158	22	0.44	385	9.5	III+	

NOTES TO TABLE 1

Columns.* (when blanks appear, data not available: SH signifies sham or N.D. or "X" - not done

Rabbit Number. Gives number of rabbit.

Air. If air was used, the number following the A expresses the air pressure in pounds/in^2 (p.s.i.) used to cool the cornea. 10 psi gave a flow rate of 16.9 l/min.

Time/W gives the time of irradiation multiplied by the average power in watts.

E(total) Joules/kg gives the energy absorbed, calculated using the specific absorption rate calculated in the text: 1 W irradiated power corresponds to a S.A.R. of 1.1 W/kg.

Peak Power W gives the peak power of the source pulses at the transmitter.

PW (Pulse Width) is the pulse duration in μ seconds.

Peak SAR (Kw/Kg) gives the calculated SAR corresponding to the peak power measured at the transmitter.

E/pulse Joules gives the energy in joules per pulse.

AvSAR W/kg gives the average SAR over the time period used for irradiation.

$_{\Delta}T^{\circ}C$ - When the measurement was available the increase in temperature (final - initial) on irradiation is recorded. Although all the data is stored on discs, financial and time constraints did not permit all termperature increases to be printed out for inclusion in the table.

Damage/% - Indicates the grade of damage (when grading was performed) and % indicates the percent of the observed area which was damaged by observation. N.D. signifies not done, and X or blank signifies that data are not available. Grades Normal and I-IV are described with criteria in the text.

TABLES

TABLE 2

COMPARISON OF THRESHOLDS FOR SPECIFIC ABSORPTION RATES AND INCIDENT IRRADIATION LEVELS FOR MILLIMETER WAVE DAMAGE FOR PULSED AND CONTINUOUS WAVE IRRADIATION

IRRADIATION CONDITIONS	EXPOSURE (SAR)	NUMBER OF RABBITS EXHIBITING CORNEAL CHANGES, OF TOTAL(T)
CONTINUOUS WAVE (CW)	0.5 W/Cm^2 (550 mW/g)	2 OF 4
PULSED (P)	0.03 W/Cm^2 (33 mW/g)	2 OF 4

FIGURE LEGENDS

Fig. 1 Overview of rabbit in holder in front of antenna in exposure chamber.

(a) View from front of antenna showing rabbit in carrier in front of round focusing antenna with eye positioned 2.5 cm behind focus of antenna.

(b) View from side of antenna showing typical view of right side of rabbit head as visible using video camera and thermographic camera.

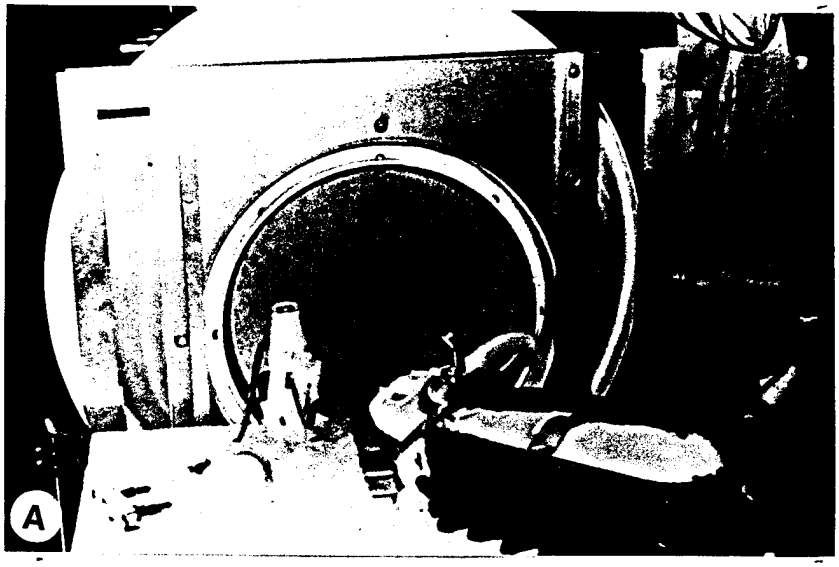

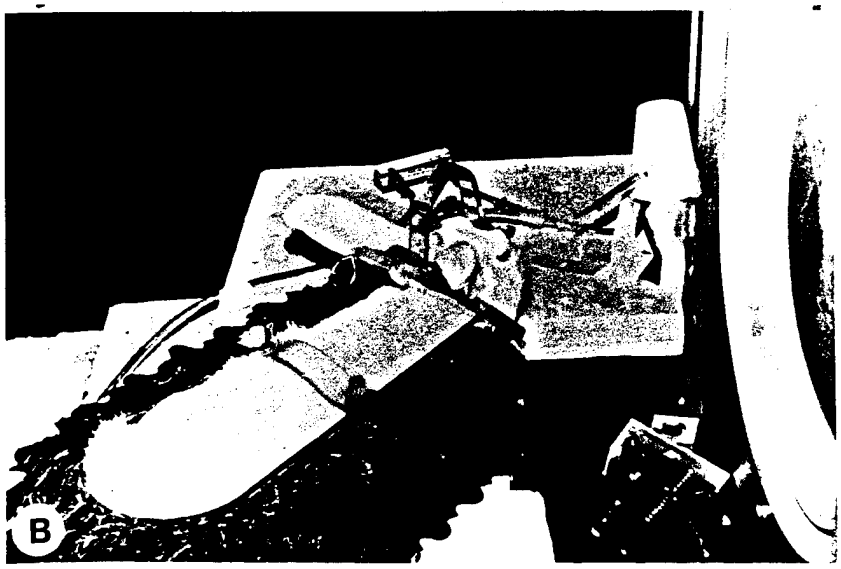

Fig. 2 Typical images and thermal profiles of rabbit head in region of the eye, obtained using different representative techniques.

(a) Photography
(b) Thermographic image using AGA Thermovision camera, range 20° Celcius.
(c) Map of temperature profiles of right side of rabbit head in the region of the eye. The temperature profiles were obtained by graphing the temperatures along lines drawn at constant vertical intervals across the map of the rabbit head temperatures.

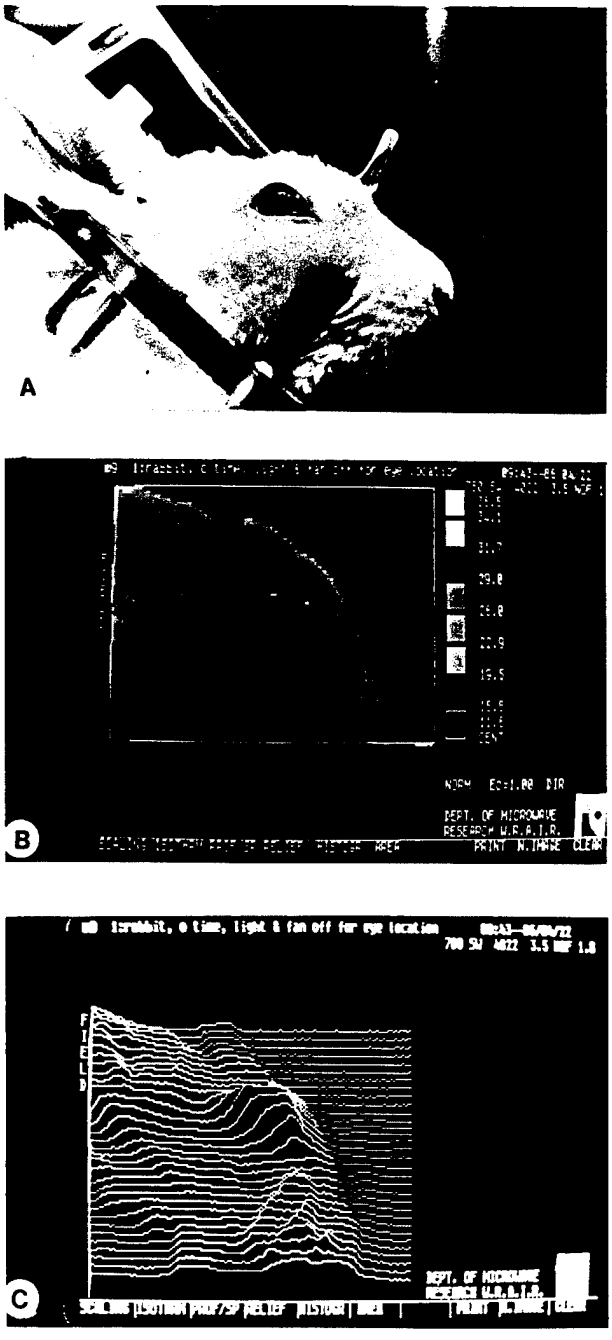

Fig. 3 Typical images and thermal profiles of rabbit head in region of the eye, obtained using different representative techniques.

(a) One horizontal profile at line 28 of the two dimensional temperature map of the right side of the rabbit head, illustrating the flattened peaks found in the corneal region.

(b) One vertical temperature profile at the division between the temporal (rear) third and the nasal (front) two-thirds of the eye (column 62).

(c) A second vertical temperature profile at the division between the nasal (front) third and the temporal (rear) two-thirds of the eye (column 75).

FIGURE 3

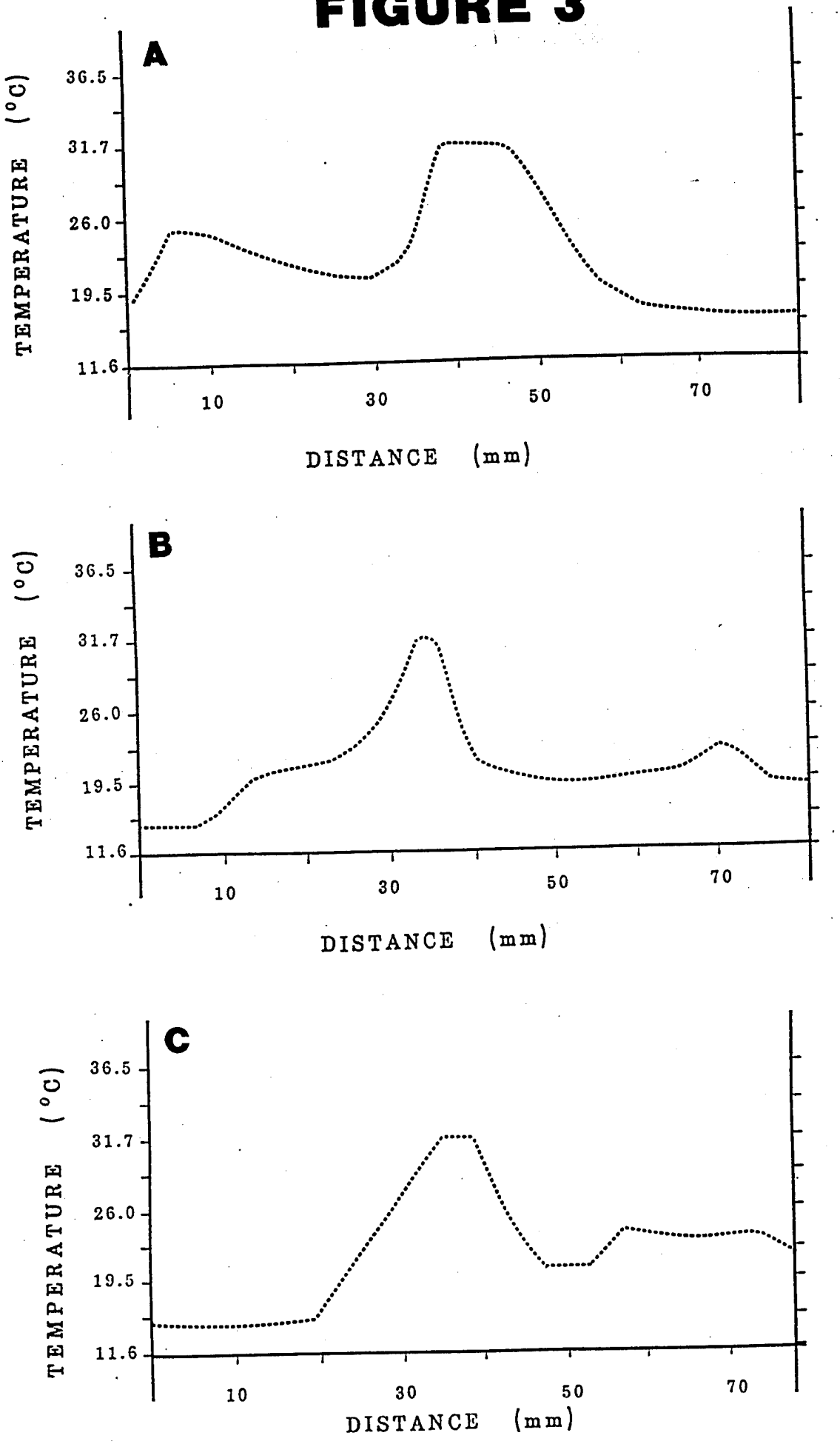
A
36.5
31.7
26.0
19.5
11.6
TEMPERATURE (°C)
10
30
50
70
DISTANCE (mm)
B
36.5
31.7
26.0
19.5
11.6
TEMPERATURE (°C)
10
30
50
70
DISTANCE (mm)
C
36.5
31.7
26.0
19.5
11.6
TEMPERATURE (°C)
10
30
50
70
DISTANCE (mm)

Fig. 4 Temperature images and graphs of profiles of the heating of the corneal phantom by the focused beam of millimeter waves from the antenna.

(a) Overall image using thermal profile plot of final-initial temperature subtraction image. The temperature differences (before irradiation subtracted from after irradiation) at each point of the thermographic image were plotted as a series of temperature profiles illustrating the spot heated by the millimeter wave beam at the beam focus.

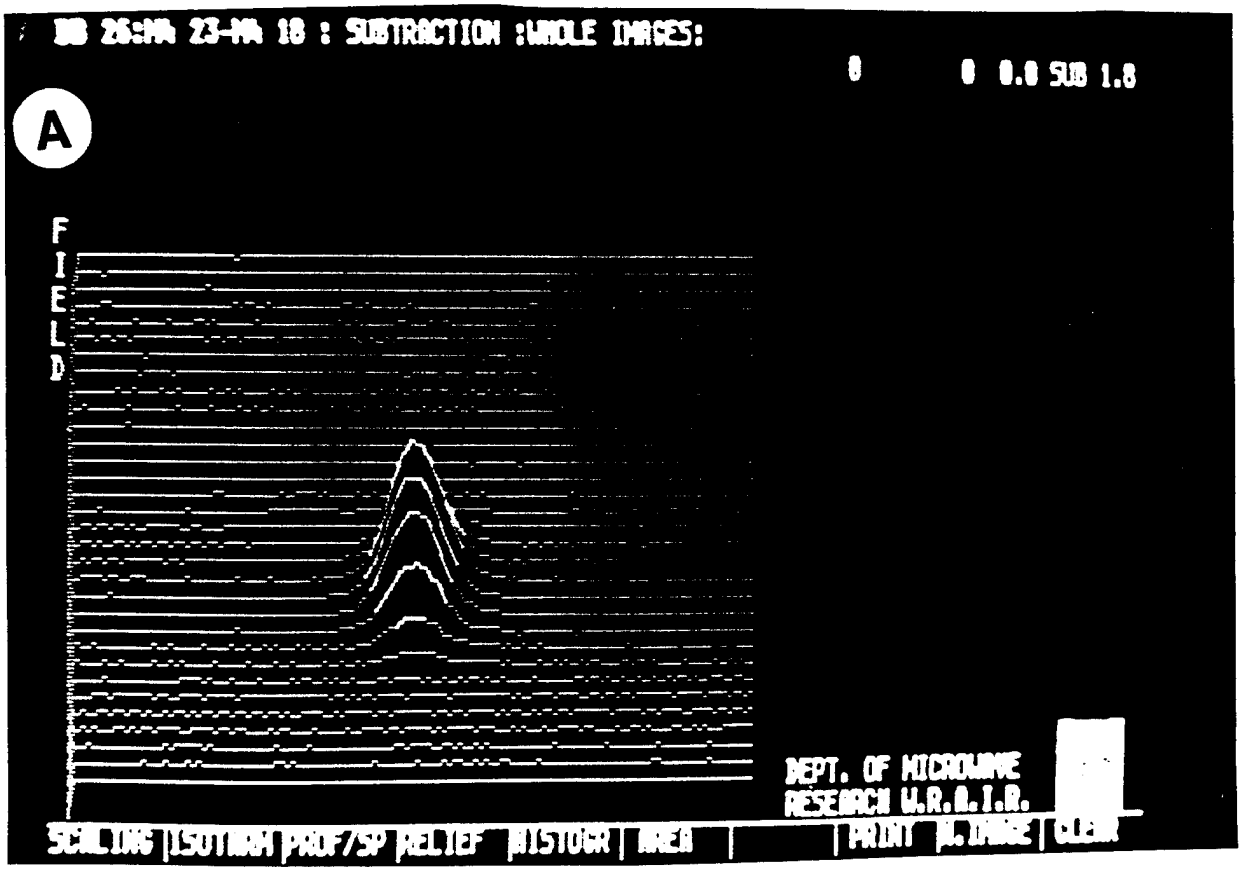

Fig. 5 Temperature images and graphs of profiles from Fig. 4 above of the heating of the corneal phantom by the focused beam of millimeter waves from the antenna.

(a) The horizontal profile of temperature differences (final-initial) through the peak at the maximum temperature reached when the cucumber at the position of the beam focus was heated by the beam at an average power of 4 W using 8 pulses of 100 μsec and 20,000 kw peak power for 2 sec total.

(b) The vertical profile through the peak point of maximum temperature difference (final - initial) reached when the cucumber was heated by the millimeter wave beam as in (a) at an average power of 4 W.

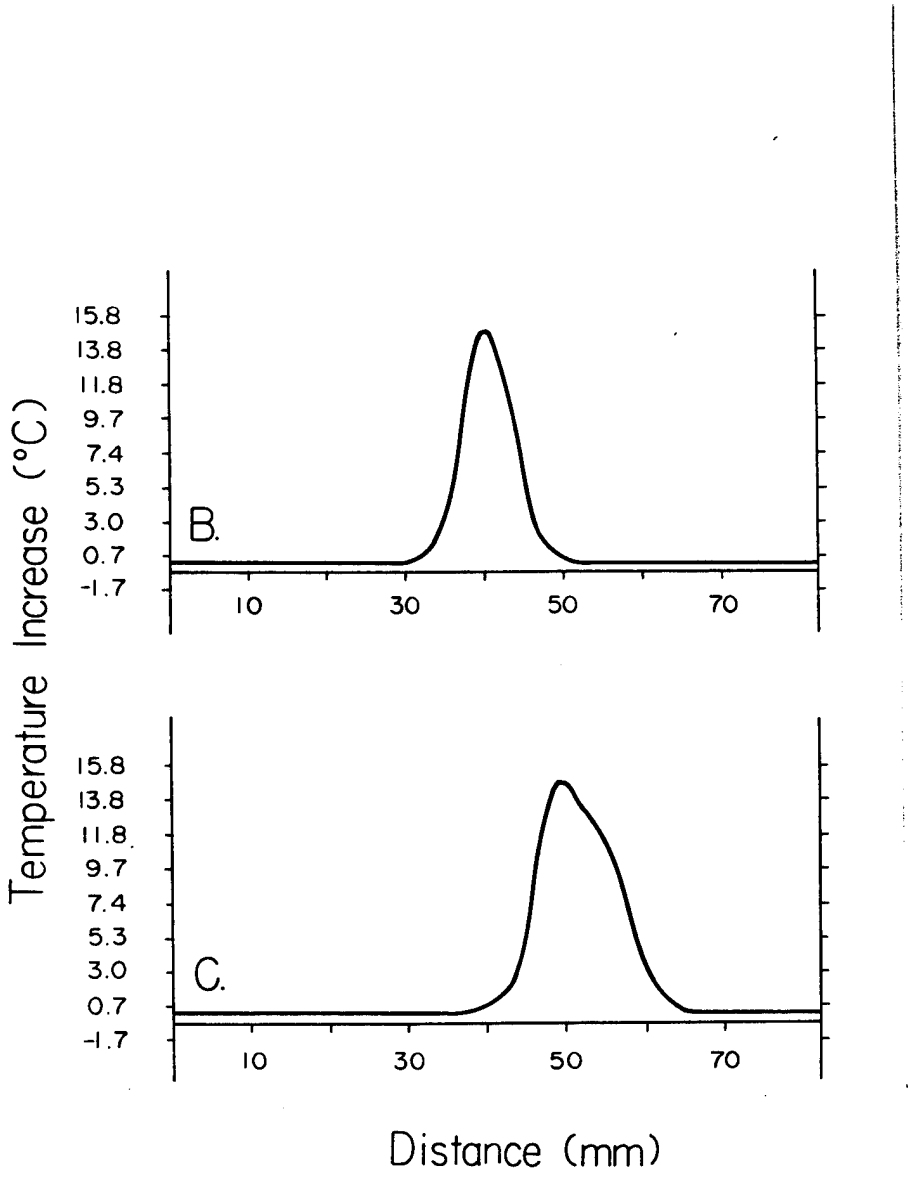

Fig. 6 Thermographic images and graphs of profiles of the temperature differences (final - initial) of the rabbit cornea heated by the focused beam of millimeter waves from the antenna.

(a) The temperature differences (before irradiation minus after irradiation) at each point of the thermographic image were plotted as a series of temperature profiles illustrating the spot heated by the millimeter wave beam at a position 2.5 cm back of the beam focus.

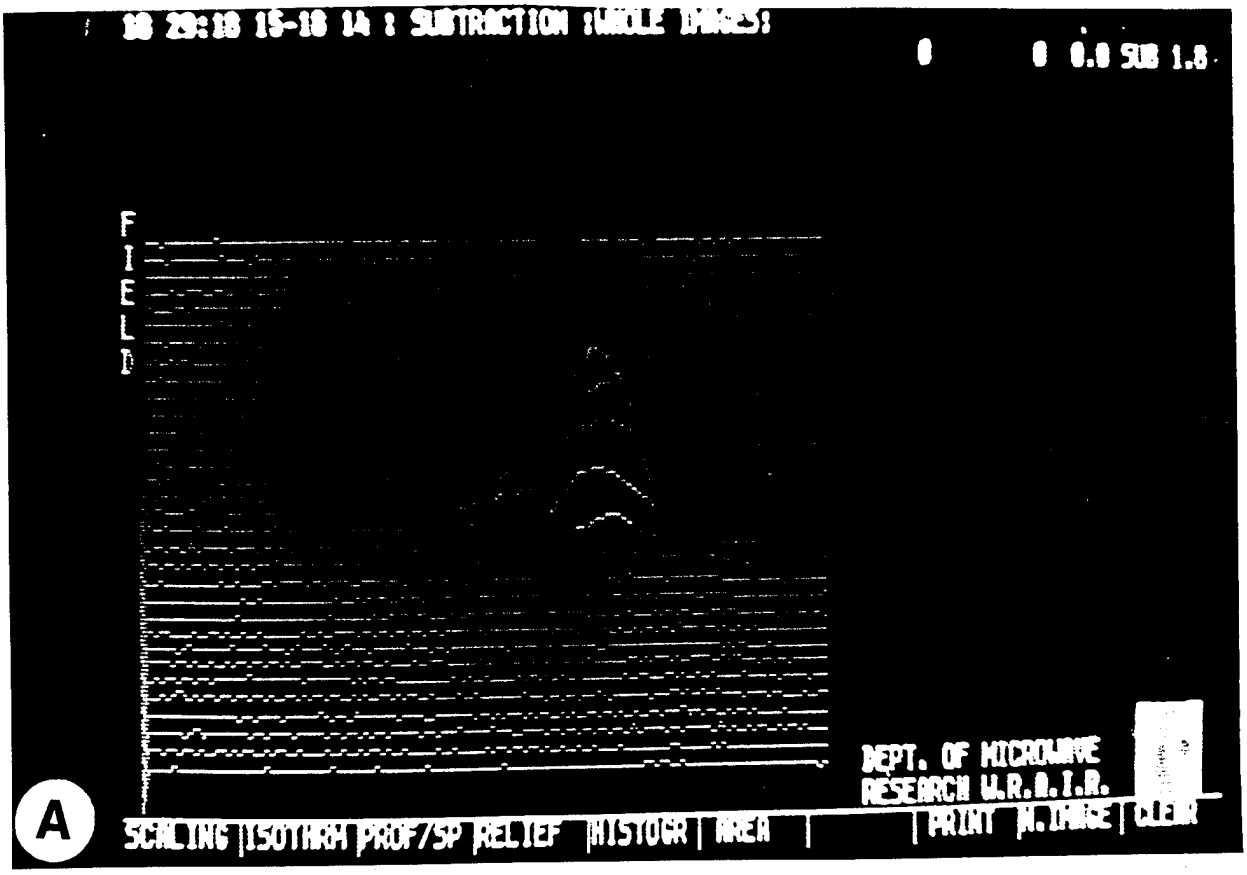

Fig. 7 Thermographic images and graphs of profiles from Fig. 6 above of the temperature differences (final - initial) of the rabbit cornea heated by the focused beam of millimeter waves from the antenna.

(a) The horizontal profile of temperature differences (final - initial) through the peak at the maximum temperature reached when the rabbit eye at the position 2.5 cm back of the beam focus was heated by the beam at an average power of 3 W using pulses of 10 μsec and 22 kw peak power for 1.5 min total.

(b) The vertical profile through the peak point of maximum temperature difference (final - initial) reached when the rabbit eye was heated by the millimeter wave beam as in (a) at an average power of 3 W.

(c) The vertical profile along a line 1/3 of the temporal-nasal distance across the rabbit eye following heating as in (b).

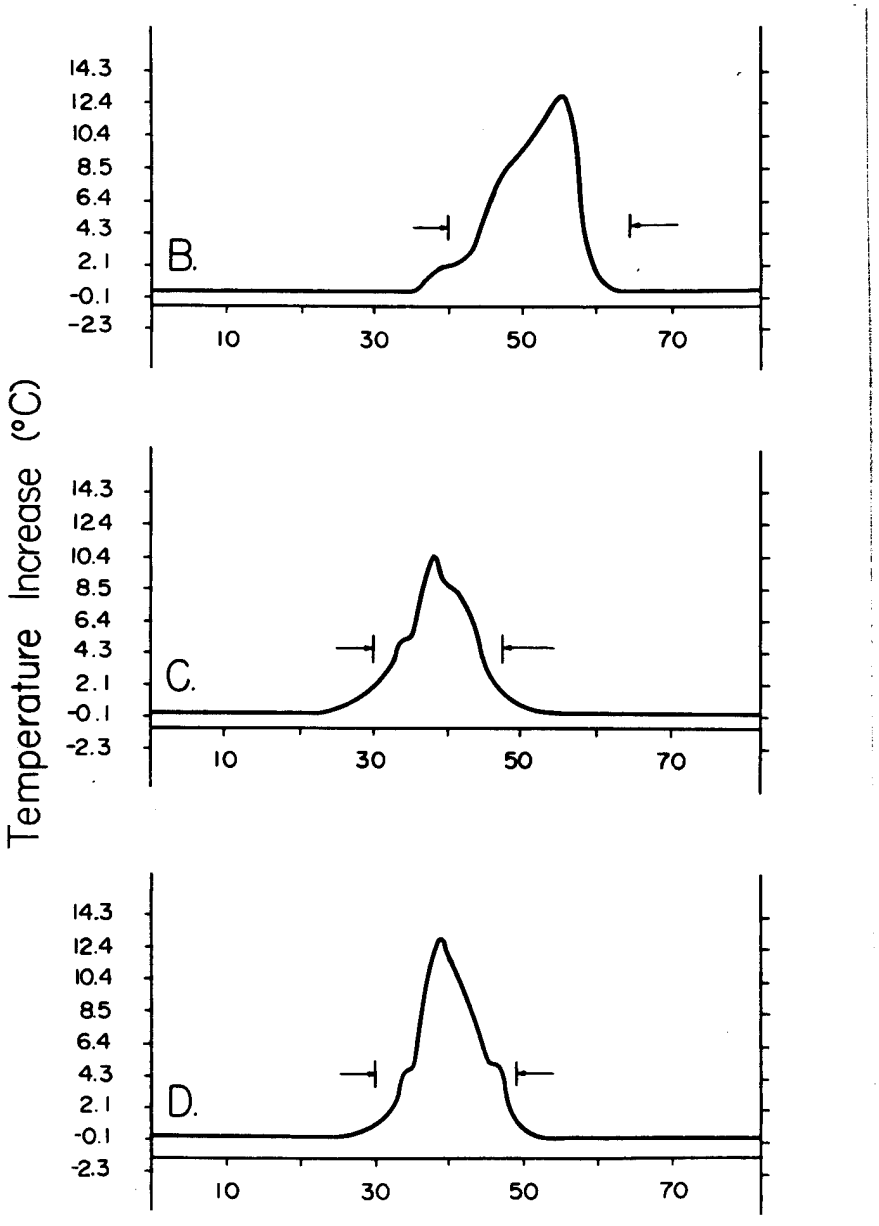

Fig. 8 Cooling of the cornea by air flow. Change of temperature (cooling) during the first ten seconds of cooling air flow at different air flow rates.

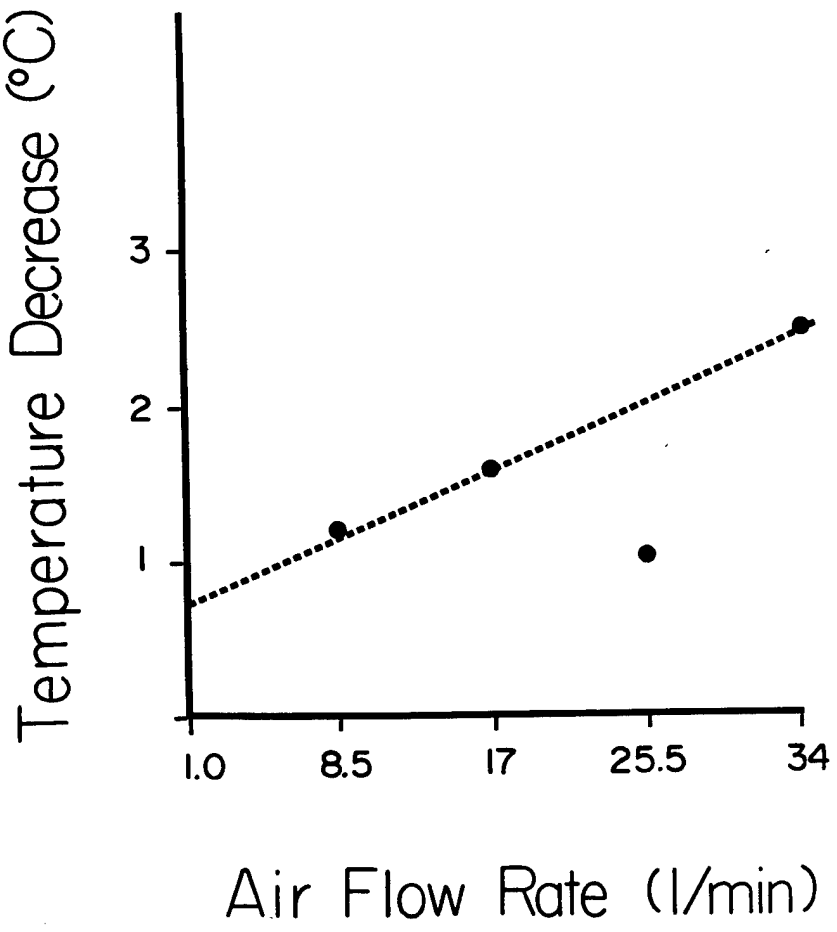

Fig. 9 Temperature as a function of power applied using continuous wave millimeter waves of frequency 35 GHz, and dependence of temperature on rates of air flow in cooling apparatus.

(a) Dependence of temperature elevation at point of maximum temperature increase on power density in W/cm^2.

(b) Dependence of the temperature elevation on the air flow rate at constant power density. Note similar slopes of lines obtained for differenti powers, showing similar decrease in temperature with increases in air flow rate.

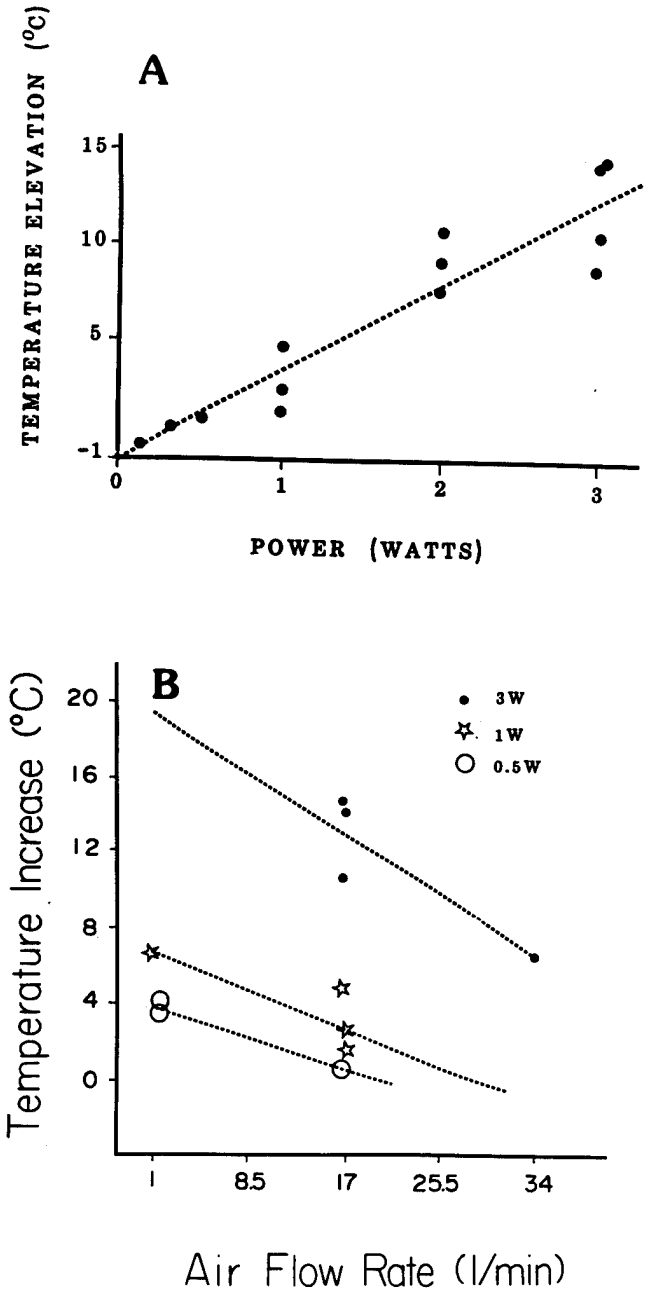

Fig. 10 Dissection of cornea for SEM, and TEM after irradiation in diagramatic view.

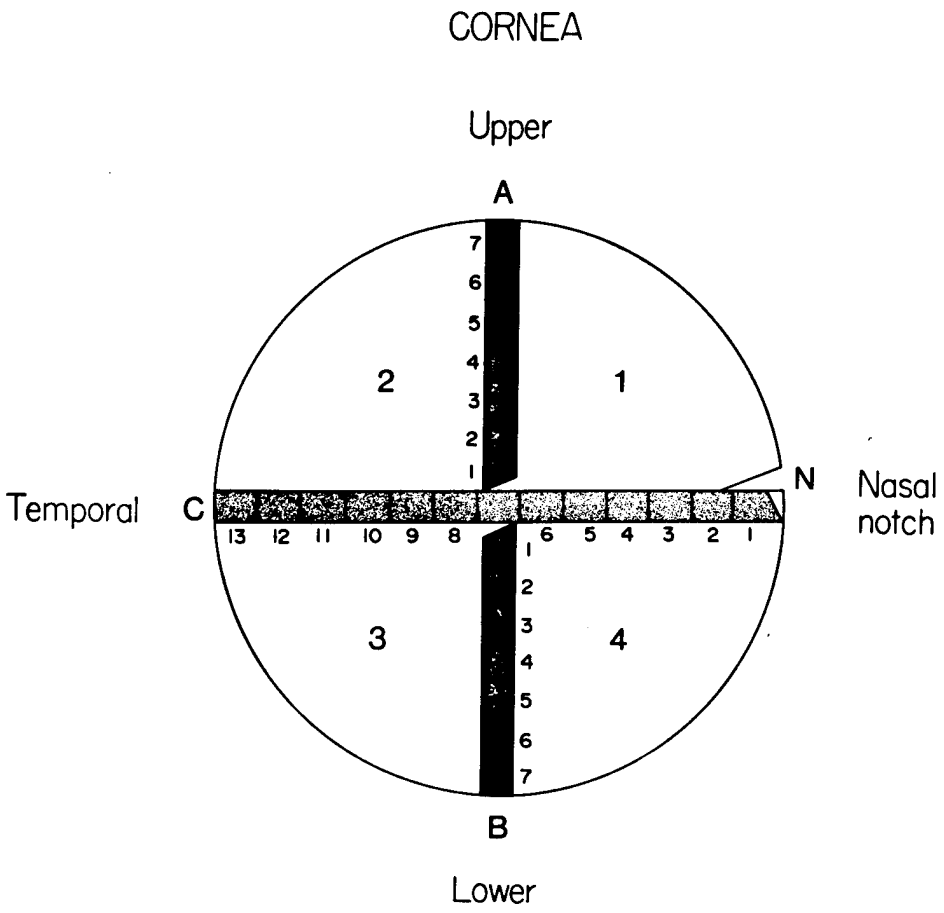

Fig. 11 Scanning electron microscopy visual library of corneal damage for millimeter wave treated rabbits.

(a) Control cornea from the left eye of a rabbit after millimeter wave exposure only on the right eye but illustrating light (1) and dark (2) cells. Note the crater like spots normally found on the surface of all cells even in normal animals. (b-d) below show increasing degrees of damage to the corneal epithelial cells seen on the right eyes of three separate millimeter wave treated rabbits.

(b) Type I - Epithelial damage in which a track-like array of single cell damage is observed. Cell damage appears due to both cell lifting and apparent heat coagulation (d). (Partial FSSD).

(c) Type II - Area of epithelial damage is increased to include apparent groups fo cells (5-8 cell total). Similar heat coagulated as in (b). (Partial FSSD).

(d) Type III - Extensive areas of epithelial damage and apparent heat coagulation are seen. Damage extends to cover standard screen area at standard 500X magnification (FSSD).

FIGURE 11

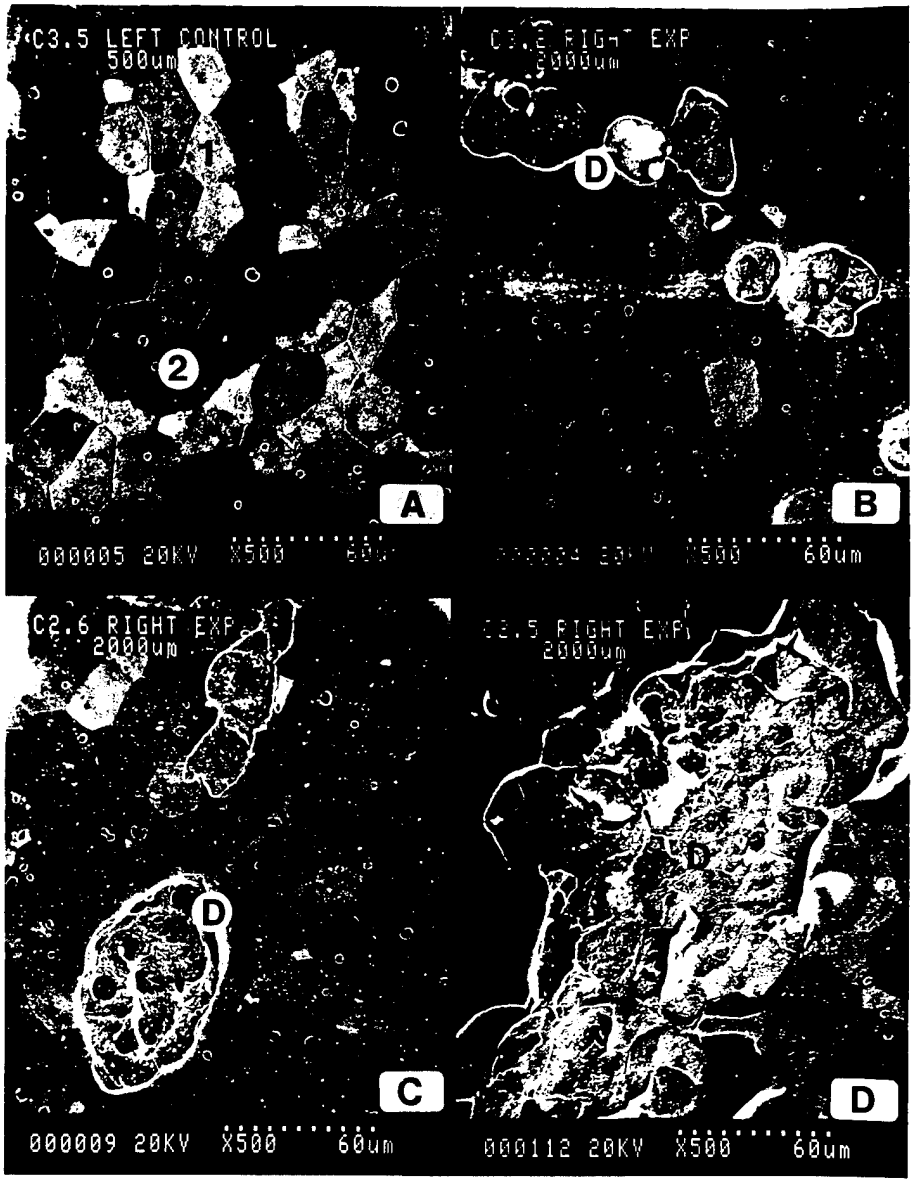
C3.5 LEFT CONTROL
500um
2
A
000005 20KV X500 60um
D
B
C2.6 RIGHT EXP
2000um
D
C
000009 20KV X500 60um
D
000112 20KV X500 60um

Fig. 12 Cross section of millimeter wave treated rabbit corneas showing varying degrees of damage in the epithelial layers (EP), the apparently normal underlying stroma (5) and where appropriate areas of degeneration (D).

(a) Occasionally the lower epithelial layers appear darkly staining, indicating more degeneration (D) than in the outer epithelial layers (EP).

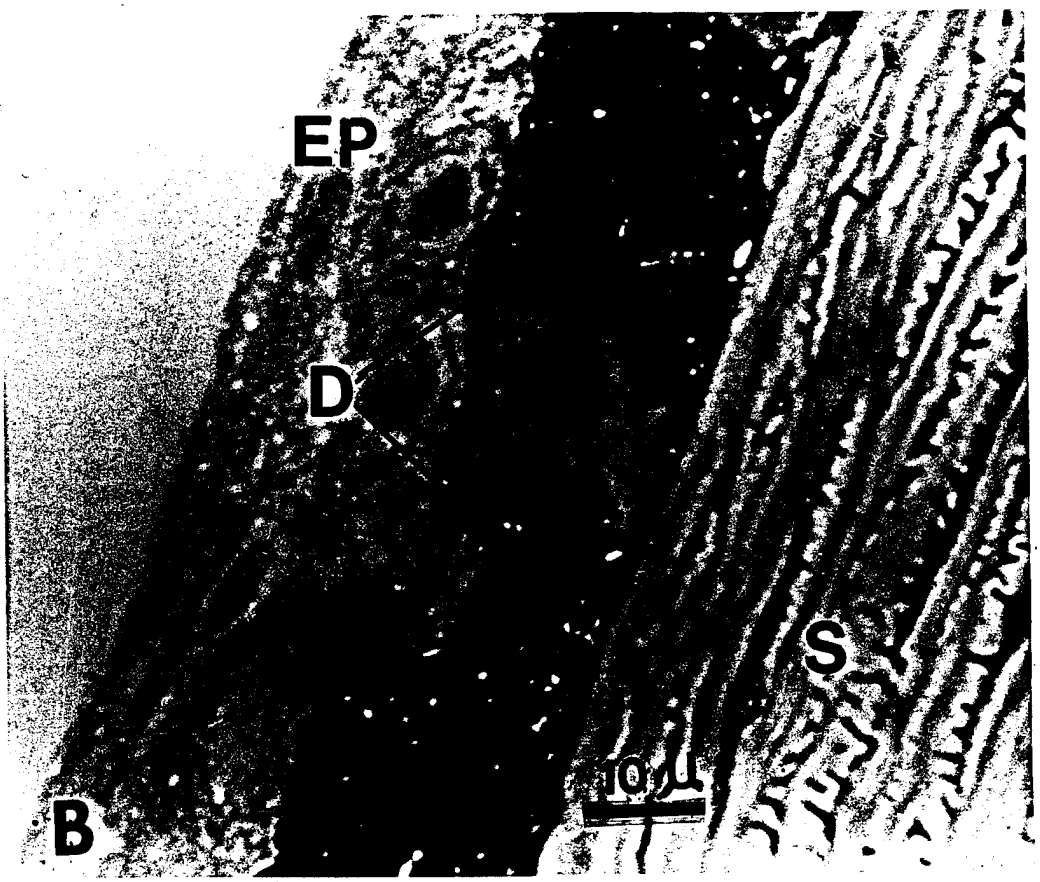

Fig. 13 Cross section of millimeter wave treated rabbit corneas showing varying degrees of damage in the epithelial layers (EP), the apparently normal underlying stroma (5) and, where appropriate, areas of degeneration (D).

(a) The outermost epithelial cells are lifting off singly as shown by arrows.

(b) In addition to single cells lifting off (—>>), there are groups of darkly staining degenerating outer epithelial cells (D).

(c) Larger areas of cornea are involved and varying degrees of degeneration of the epithelial layers is seen; in some areas varying numbers of epithelial cell layers are lost, at places exposing the stroma (EX).

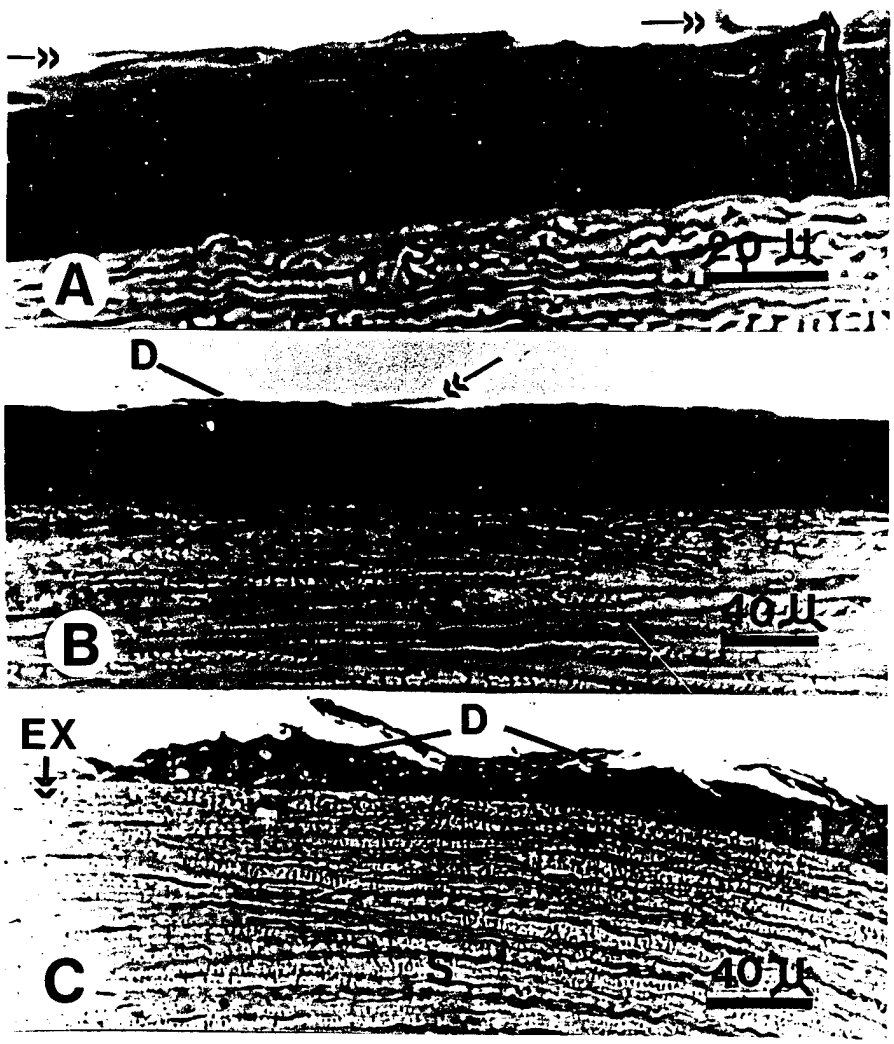

Fig. 14 Thermographic images of modelling of accidental exposure to millimeter waves.

(a-b) Thermographic imaging indicated a maximum increase in temperature in the irradiated area of 9.5°C, from the normal rabbit corneal temperature of approximately 34.5°C. Severe damage was caused by the 0.18 sec exposure to 158 pulses of 20 μsec, at a spatial peak SAR of 22 KW/g.

Each of 2 rabbits moved their heads and closed the irradiated eye after irradiation. Thermographic imaging indicated an increased temperature, to no more than 44° C, from the normal corneal temperature of 34.5° C.

(a) Subtraction image of rabbit 118: control (of line) is subtracted from image at 0.1 sec of irradiation.

(b) For subtraction image temperature of spot identified, by crossed lines at highest peak of temperature elevation.

FIGURE 14

A


89 12: 89 4-89 3 : SUBTRACTION :WHOLE IMAGES:
-2.9
3.4
6.5
1892 PIX. (0 D, 8300 PIX.)= 0 D
89 4:Tmin= 33.7 Tmax= 49.7
89 3:Tmin= 33.7 Tmax= 49.7

B

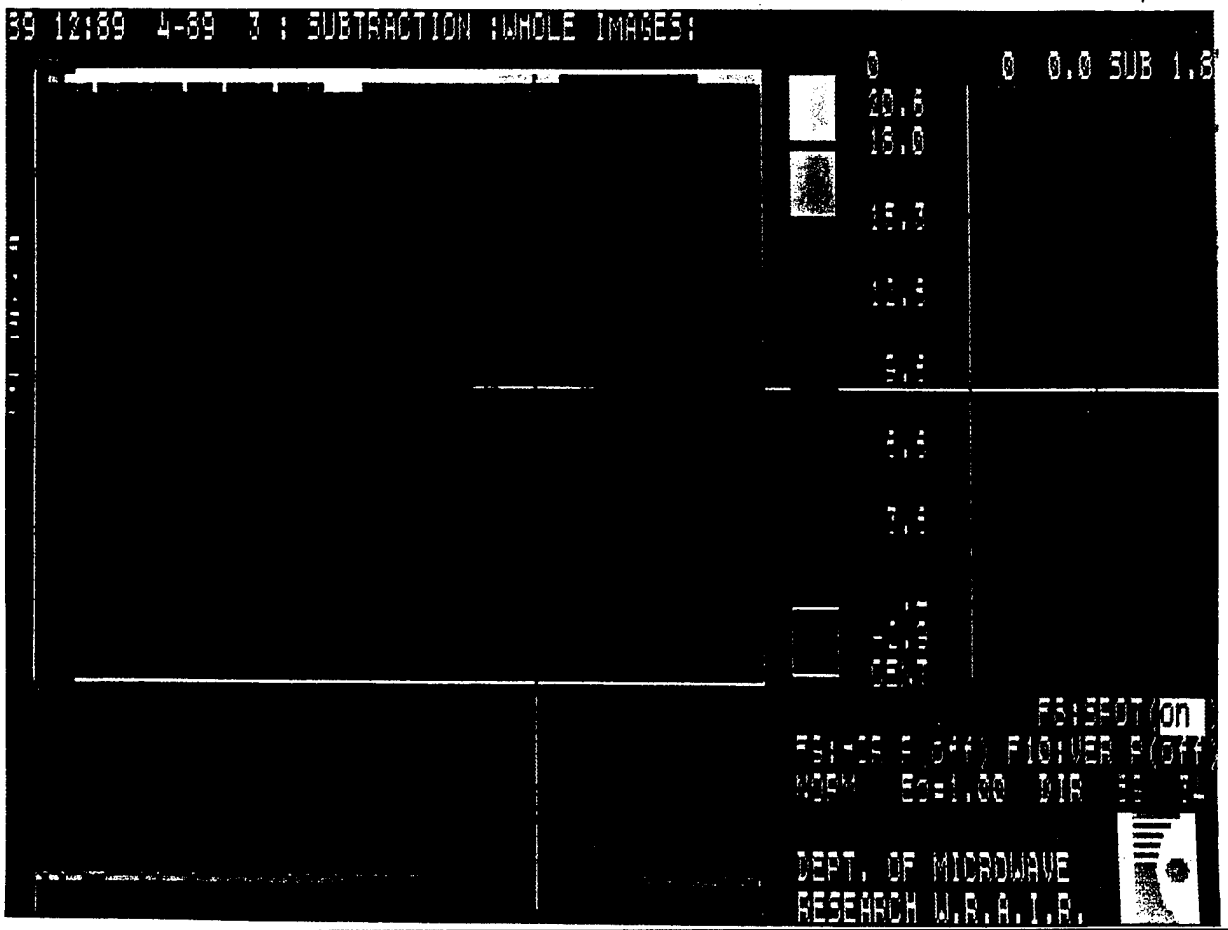
89 12:89 4-89 3 : SUBTRACTION :WHOLE IMAGES:
0 0 0.0 SUB 1.6
20.6
16.0
16.7
F5:SPOT on
DEPT. OF MICROWAVE
RESEARCH W.R.A.I.R.

Fig. 15 Scanning electron microscopy of the epithelium surface of the cornea damaged to simulate accidental exposure to millimeter waves.

(a-c) In the irradiated area, damage occurred in an oval area positioned across the border between quadrant 1 and 4, with the border equally dividing the oval damaged area along its short axis. (Fig. ABC). Several other point areas of damage occurred at pits in adjacent areas, and peculiar tracks not found in unirradiated samples were also found. Magnifications are indicated on the scanning electron microsope pictures by the scale bar:

epithelial surface (a) a portion of the large approximately oval area of damage from quadrant 1.
(b) a higher magnification view of (1).
(c) an area of pit damage in quadrant 1.

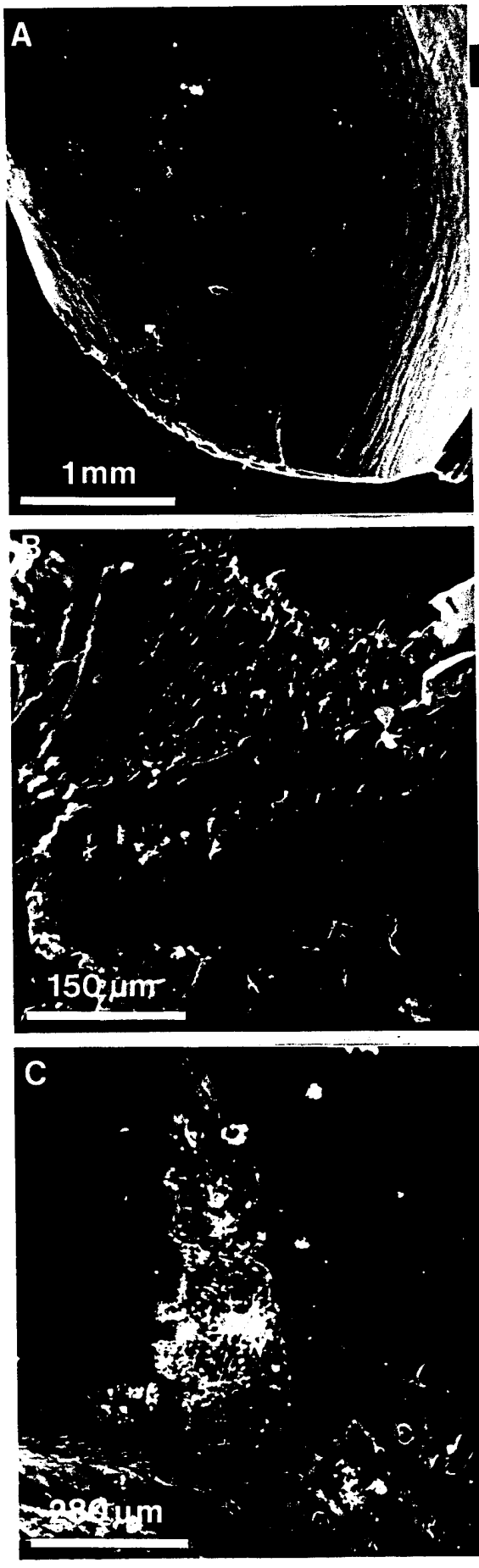

FIGURE 15

Fig. 16 Scanning electron microscopy of the endothelial surface of the cornea damaged to simulate accidental exposure to millimeter waves.

At the endothelial surface an unusual bulge in the endothelial cellular sheet may indicate the force or pressure which was exerted by the exposure to the pulsed millimeter wave beam. That this is a bona fide bulge was shown by its behaviour on exposure to the electron beam in the scanning microscope, which produced a dimple in the bulge.

(a) A portion of the approximately oval bulge from quadrant 2.
(b) The same bulge shown in Fig. 5 after depression by the force of the electron beam.
(c) The contour map of (6) illustrating its central depression caused by the electron beam.

FIGURE 16

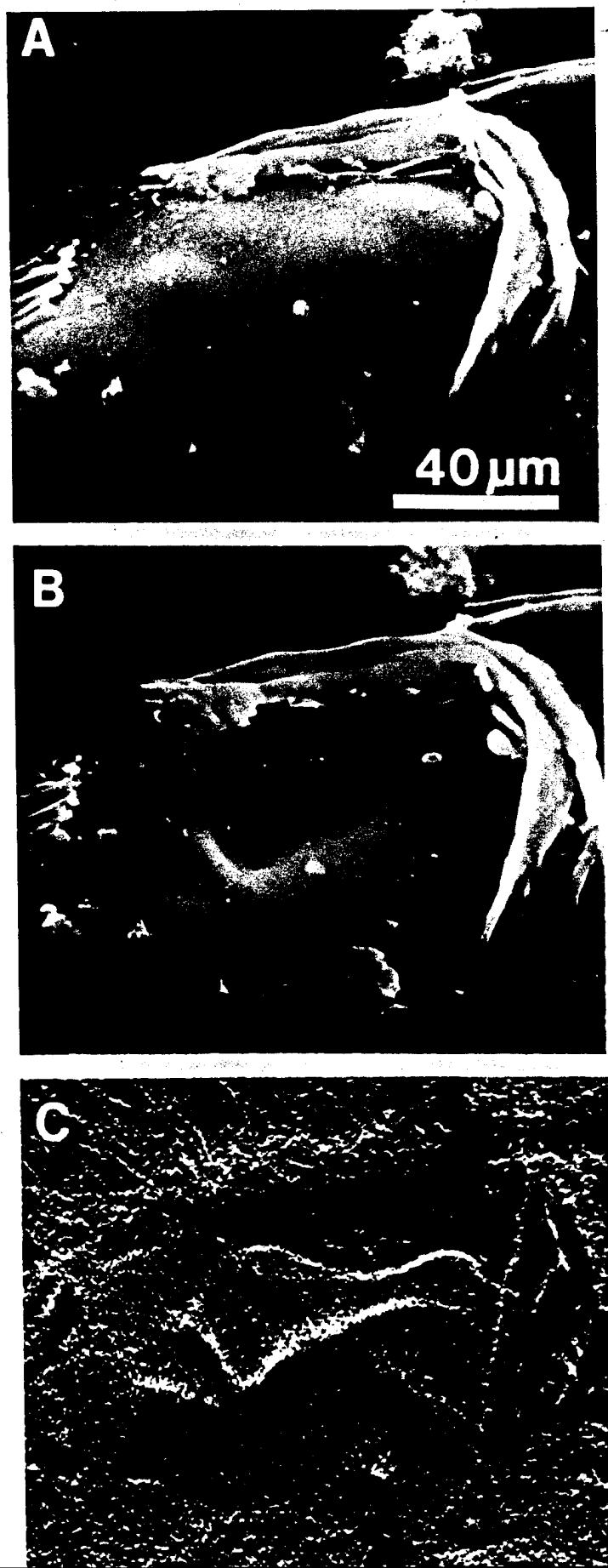

Fig. 17 Light microscopy of damaged area fixed after exposure to millimeter waves irradiation as described in figures 15 and 16 above.

(a-e) In the oval area no epithelial cells were seen covering the oval area, (Fig. A) while at the borders of the area finger-like projections of the corneal stroma covered with one layer of epithelial cells instead of the usually multilayered structure of the epithelium. The stroma has apparently been disrupted so that it appears to have flowed or snapped back, like a rubber band suddenly released from tension, to form the underlying support of these cells, while retaining its layered structure:

A. Central region of lesion showing complete removal of epithelium from stromal surface.

B. Montage of section through the strip at the border of the junction between quadrants 1 and 4, illustrating (top of montage) finger-like projections of the corneal stroma covered with one layer of epithelial cells instead of the usual multilayered structure of the epithelium. The stroma has apparently been disrupted so that it appears to have flowed or snapped back, like a rubber band suddenly released from tension, to form the underlying support of these cells, while retaining its layered structure.

C. A higher magnification view of (8) showing the finger-like projection with its single layer of epithelium surrounding the disrupted layers of stroma.

D. An area near the projections in (8) and (9) shows the multilayered epithelium which in places is thinned due to the outward projections of stromal material, and illustrates the large lakes of fluid of different refractive index from the surrounding stroma. These lakes would interfere significantly with vision because of the light scattering and reflections (due to differences in refractive index they would cause in the affected area of the cornea.

E. The endothelial side shown below in this montage, also appears to have been damaged (layer disruption at left of photo), and projects outward from the stromal surface.

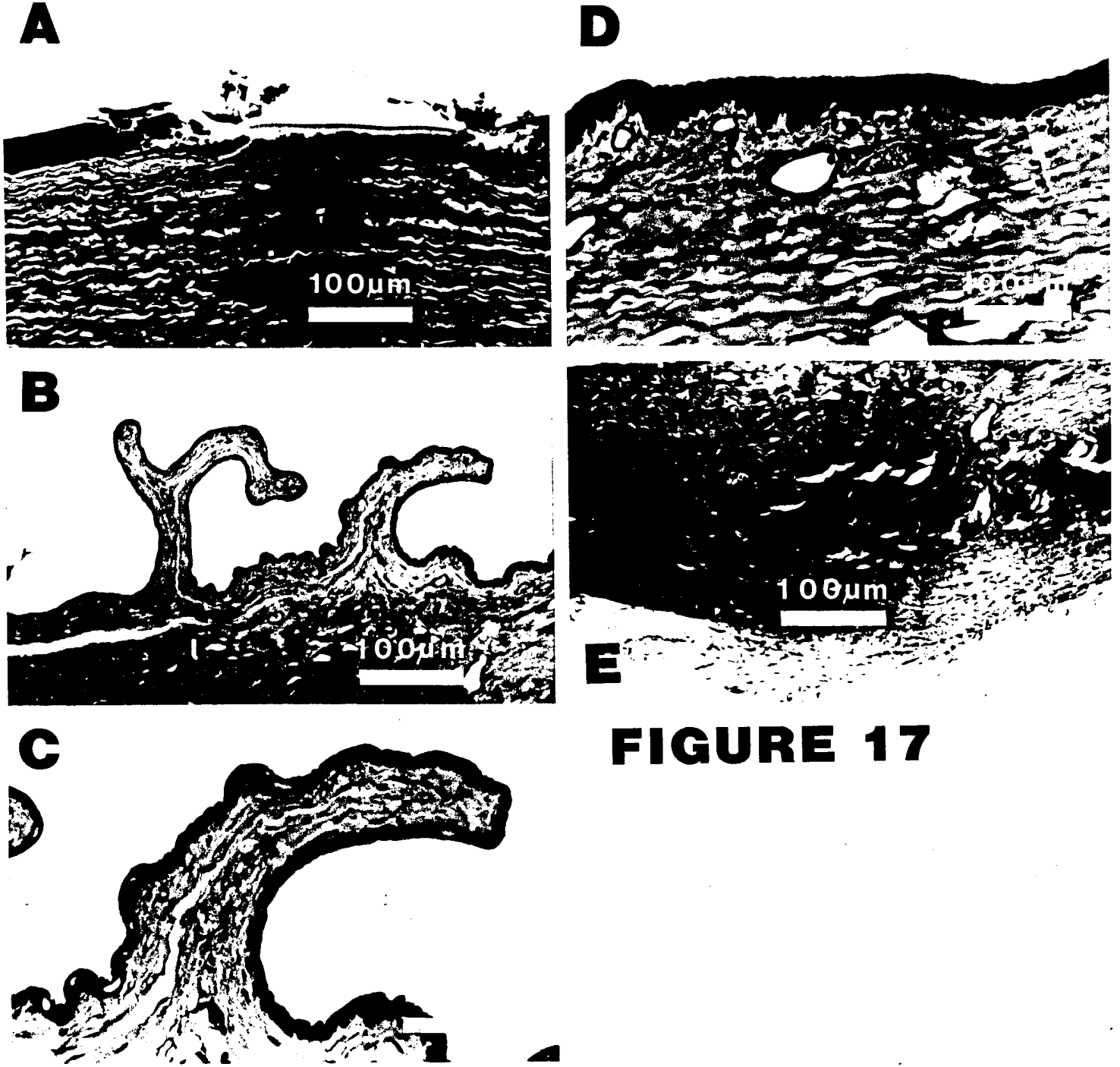

FIGURE 17